WL-TR-91-4121

COMPUTED TOMOGRAPHY ANALYSIS OF CASTINGS

Richard H. Bossi
Gary E. Georgeson

Boeing Aerospace & Electronics
P.O. Box 3999
Seattle, WA 98124

January 1992

Interim Report for Period March 1990 - December 1990

MATERIALS DIRECTORATE
WRIGHT LABORATORY
AIR FORCE SYSTEMS COMMAND
WRIGHT-PATTERSON AIR FORCE BASE, OHIO 45433-6533

NOTICE

When Government drawings, specifications, or other data are used for any purpose other than in connection with a definitely Government-related procurement, the United States Government incurs no responsibility or any obligation whatsoever. The fact that the government may have formulated or in any way supplied the said drawings, specifications, or other data , is not to be regarded by implication, or otherwise in any manner construed, as licensing the holder, or any other person or corporation: or as conveying any rights or permission to manufacture, use, or sell any patented invention that may in any way be related thereto.

This report is releasable to the National Technical Information Service (NTIS). At NTIS, it will be available to the general public, including foreign nations.

This technical report has been reviewed and is approved for publication.

CHARLES F. BUYNAK
Nondestructive Evaluation Branch
Metals and Ceramics Division

TOBEY M. CORDELL, Chief
Nondestructive Evaluation Branch
Metals and Ceramics Division

FOR THE COMMANDER

DR. NORMAN M. TALLAN, Director
Metals and Ceramics Division
Materials Directorate

If your address has changed, if you wish to be removed from our mailing list, or if the addressee is no longer employed by your organization please notify WL/MLLP , WPAFB, OH 45433-6533 to help us maintain a current mailing list.

Copies of this report should not be returned unless return is required by security considerations, contractual obligations, or notice on a specific document.

REPORT DOCUMENTATION PAGE

Form Approved
OMB No. 0704-0188

1. AGENCY USE ONLY (Leave Blank)	2. REPORT Date	3. REPORT TYPE AND DATES COVERED
	January 2, 1992	Interim Mar 90-Dec 90

4.. TITLE AND SUBTITLE

Computed Tomography Analysis of Castings

5. FUNDING NUMBERS

F33615-88-C-5404
PE: 63112F
PR: 3153
TA: 00
WU: 06

6. AUTHOR(S)

Richard H. Bossi

Gary E. Georgeson

7.. PERFORMING ORGANIZATION NAME(S) AND ADDRESS(ES)

Boeing Defense and Space Group
P.O. Box 3999
Seattle, WA 98124-2499

8. PERFORMING ORGANIZATION REPORT NUMBER

9. SPONSORING/MONITORING AGENCY NAME(S) AND ADDRESS(ES)

Charles F. Buynak (513-255-9802)
Wright Laboratory (WL/MLLP)
Materials Directorate
Wright-Patterson AFB, OH 54533-6533

10. SPONSORING/MONITORING AGENCY REPORT NUMBER

WL-TR-91-4121

16. SUPPLEMENTARY NOTES

12a. DISTRIBUTION/AVAILABILITY STATEMENT

Approved for Public Release; Distribution is unlimited.

12b. DISTRIBUTION CODE

13. ABSTRACT (Maximum 200 words)

Under a preliminary testing task assignment of the Advanced Development of X-ray Computed Tomography Application program, computed tomography (CT) has been studied for its potential use in the analysis of castings. Because CT is quantitative, it offers a nondestructive evaluation (NDE) capability that can be used for engineering analysis, accurate dimensional measurement and for reconstructing three-dimensional models of cast components using Stereolithography.

CT sensitivity to anomaly sizes has been measured by the use of image quality indicators. The sensitivity of a CT system, as a function of object size and system operating parameters, can be established and monitored. The three-dimensional location and definition of flaws, obtained from CT evaluation of castings, have been input into finite element engineering models to analyze the performance as a function of the casting condition. A significant cost savings in the manufacture of castings and their increased aerospace application is possible if CT evaluation and fitness-for-service criteria are used. Dimensional measurements with excellent accuracies and precision better than 0.050 mm (0.0012 inch) have been demonstrated. The data sets from CT scanning have been converted to CAD/CAM files and input to a Stereolithography system to build a 3D plastic model of a part.

14. SUBJECT TERMS

Computed Tomography (CT); Castings; Image Quality Indicators (IQI); defect; defect sensitivity; finite element analysis (FEA); phantom; Stereolithography; modulation; noise; dimensional measurement; gap measurement

15.NUMBER OF PAGES

37

16. PRICE CODE

17. SECURITY CLASSIFICATION OF REPORT	18. SECURITY CLASSIFICATION OF THIS PAGE	19. SECURITY CLASSIFICATION OF ABSTRACT	20. LIMITATION OF ABSTRACT
Unclassified	Unclassified	Unclassified	UL

NSN 7540-01-280-5500

Standard Form 298 (Rev. 2-89)
Prescribed by ANSI Std. Z39-18
298-102

TABLE OF CONTENTS

LIST OF FIGURES

LIST OF TABLES

SUMMARY

Under a preliminary testing task assignment of the Advanced Development of X-ray Computed Tomography Application program, computed tomography (CT) has been studied for its potential use in the analysis of castings. Because CT is quantitative, it offers a nondestructive evaluation (NDE) capability that can be used for engineering analysis, accurate dimensional measurements and for reconstructing three-dimensional models of cast components using stereolithography.

CT sensitivity to anomaly sizes has been measured by the use of image quality indicators. The sensitivity of a CT system, as a function of object size and system operating parameters, can be established and monitored. The three-dimensional location and definition of flaws, obtained from CT evaluation of castings, have been input into finite element engineering models to analyze the performance as a function of the casting condition. A significant cost savings in the manufacture of castings and their increased aerospace application is possible if CT evaluation and fitness-for-service criteria are used. Dimensional measurements with excellent accuracies and precision better than 0.050 mm (0.0012 inch) have been demonstrated. The data sets from CT scanning have been converted to CAD/CAM files and input to a Stereolithography system to build a 3D plastic model of a part.

ACKNOWLEDGEMENTS

Dave Cruikshank, Gary Matack and Candice Snydar of Boeing are acknowledged for their efforts in the acquisition of IGES files and FEA analysis. James Nelson and Jud Geiger of Boeing are acknowledged for their effort on the dimensional measurements of small gaps. Rick Baczuk, Dan Belsvig and Alan Crews of Boeing are acknowledged for their effort on CT data conversion to CAD/CAM. Special thanks are due to Charles Fischer of the University of Kentucky, Wenner-Gren Laboratory for the creation of the Stereolithography model.

DISCLAIMER

The information contained in this document is neither an endorsement nor criticism for any X-ray imaging instrumentation or equipment used in this study.

1.0 INTRODUCTION

The goal of the Advanced Development of X-Ray Computed Tomography Applications demonstration (CTAD) program is to evaluate applications for which computed tomography (CT) can provide a cost-effective means of evaluating aircraft/aerospace components. The program is task assigned so that specific CT applications or application areas can be addressed in separate task assigned projects. This interim report is the result of a task assignment study. Three categories of task assignments are employed in the program: 1) preliminary tests, where a variety of parts and components in an application area are evaluated for their suitability to CT examinations for their inspection; 2) final tests, where one or a few components are selected for detailed testing of CT capability to detect and quantify defects; and 3) demonstrations, where the economic viability of CT to the inspection problem are analyzed and the results presented to government and industry. This interim report is in addition to the interim report "X-Ray Computed Tomography for Full-Scale Castings" [1]. References [2-7] are other CTAD reports on various application areas.

1.1 X-ray Computed Tomography

X-ray computed tomography (CT) is a powerful nondestructive evaluation technique that was conceived in the early 1960's and has been developing rapidly ever since. CT collects X-ray transmission data from many angles around the component to digitally reconstruct a map of the relative X-ray linear attenuation coefficient of small interior volume elements and view them as cross sectional images. The clear images of an interior plane of an object are achieved without the confusion of superposition of features often found with conventional film radiography. CT provides quantitative information about the material/density and dimensions of the features imaged. This digital data can be used for engineering analysis.

1.2 Scope and Objectives

The task assignment, designated "Task 6 - Full Scale Castings," is a preliminary testing task directed at the inspection of full scale cast components. This report covers the use of CT measurements for quantitative engineering analysis of castings. Four areas are considered: CT sensitivity, engineering analysis, dimensional measurements and stereolithography. The application of CT to full-scale castings and the economic incentives to implement CT are discussed in a separate report [1].

The overall objective of this report is to evaluate the applicability of using CT for the analysis of cast components. By using the quantitative, three-dimensional capability of CT for examination, it is hoped that the casting evaluation criteria could be revised in order to reduce the high rejection rates commonly found in many aerospace castings.

The Task 6 test plan included the acquisition of test samples, CT scanning, and data evaluation. It also included designing and using CT image quality indicators for defect sensitivity measurements. Defect sensitivity studies were conducted which correlated signal-to-noise values and modulation with the ability to resolve small voids.

2.0 CT SENSITIVITY

2.1 CT Image Quality Indicators (IQIs)

Image quality indicators (IQI's) provide a means of quantitatively assessing the performance of imaging systems. For radiography, the plaque penetrameter has been the standard [8]. An IQI for use in CT casting studies has also been devised that is very similar. Figure 2.1-1 is a photograph of the three pieces of a CT IQI assembly. The CT IQI is composed a 19 mm (0.75 inch) diameter disk of selectable thickness, containing 2 or 3 holes, with cylindrical shims of the same material on both sides of the thin disk. The IQI thus contains cylindrical voids of a height equivalent to the disk thickness and diameters of the holes. For this study, the disk thickness was 0.25 mm (0.010 inch) and the three hole diameters were 1.0 mm (0.040 inch), 0.50 mm (0.020 inch) and 0.25 mm (0.010 inch). These equate to volumetric void sizes of 0.2, 0.05, and 0.012 mm^3 respectively. In order for the IQI to be useful, the CT slice must be taken such that it covers the plane of the disk. The CT slice may be thicker than the disk and still be sensitive to the voids. The Appendix discusses the CT IQI.

Figure 2.1-1 Photograph of the three pieces of a CT IQI for casting studies (PID #000902).

When one of these IQIs is placed in the scan plane of the casting during a CT test, a direct measure of volumetric feature size for the CT image is possible. For experimental studies, a series of concentric rings was fabricated from aluminum which fit around the IQI. These rings are shown in Figure 2.1-2. Measurements of detectability as a function of the number of concentric rings can be used to monitor system sensitivity.

Figure 2.1-2 Photograph of aluminum concentric rings (PID #000303).

2.2 Part Thickness Effects on Defect Sensitivity

For any given CT system, the image resolution will depend (to the first approximation) on the X-ray optics of the design [9-11]. The noise, however, will be affected by the operating parameters such as slice thickness, scan time, and X-ray energy. As the geometry of the object changes, so does the noise. An increase in the X-ray path length will cause an increase in the noise in the image. The theoretical effect of path length on the signal-to-noise ratio (SNR) in a CT image is approximated by:

$$SNR \propto \mu[nte^{-2\mu R}]^{1/2} \qquad 2\text{-}1$$

where μ is the linear attenuation coefficient, n is number of photons detected without an object present, t is the integration time and R is the path length [12,13]. The noise is given by:

$$Noise = 100/SNR \qquad 2\text{-}2$$

where the noise is in percent.

Figure 2.2-1 shows the experimental and theoretical curves for noise, in percent, as a function of path length for a CT system. The path length in the experimental case has been changed by increasing the number of concentric rings of the Figure 2.1-2 aluminum ring set that are used. The experimental data is taken at two different X-ray energies. The noise measurement is obtained by selecting a region of interest and measuring the spread of the CT values. As the size of the object increases (which is produced by adding rings), the X-ray path length increases, the noise level increqases, and the image becomes grainier. The theoretical and empirical curves have a similar shape. The theoretical curve has been normalized to the experimental values.

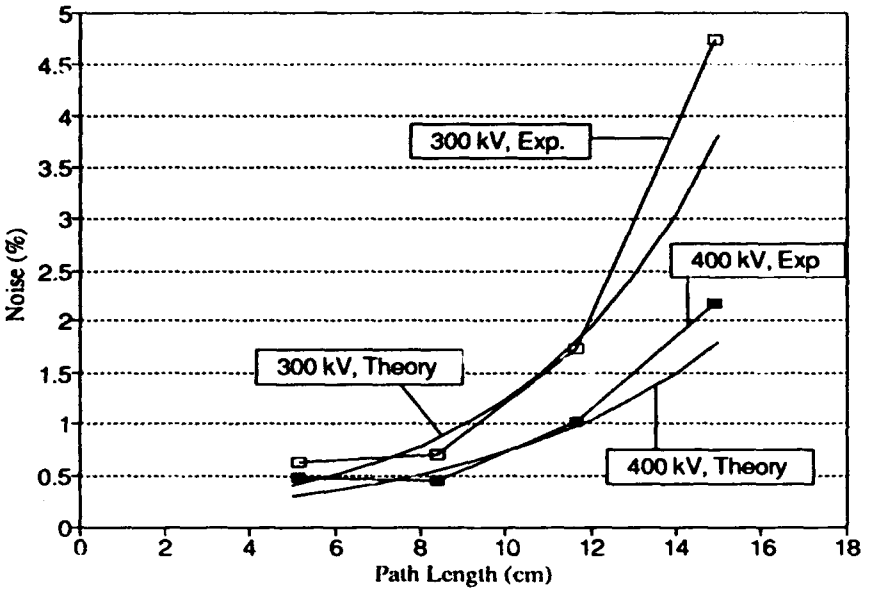

Figure 2.2-1 Noise versus path length curves for CT.

The sensitivity to small defects as a function of X-ray path length was examined using measurements from the CT IQI at the center of the rings. Line plots through the CT image of the voids provide a numeric value for the image modulation. In order for a feature (void) to be detected, the modulation must be greater than the noise.

Figure 2.2-2 shows the ratio of the modulation of the 0.2 and 0.05 mm^3 voids to the noise in the CT image as a function of the object size (path length) at two X-ray energies. As in the previous case, the path length (and thus, the noise) has been changed by adding rings. An increase in noise due to path length causes the modulation-to-noise ratio to decrease. The higher energy CT scans show a greater modulation-to-noise ratio. This should be due to the increase in signal strength which reduces noise in the image. At low path lengths for the 400 kV case, there is an improvement in the ratio for a small increase in the path length. This is apparently due to the small decrease in noise as path length increases for the 400 kV case (shown in Figure 2.2-1) at 8 cm path length combined with a slight increase in modulation as path length increased for this particular industrial CT system. The Figure 2.2-2 plot allows one to predict the sensitivity that can be achieved as a function of the amount of material present. Obviously, to improve the detectability of fine detail, one needs to increase the modulation or decrease the noise.

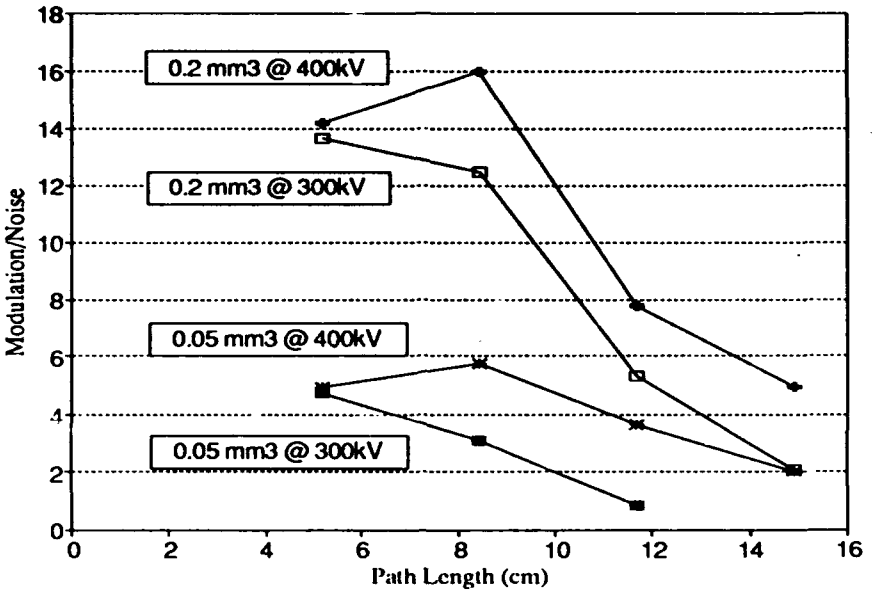

Figure 2.2-2 Modulation/noise versus path length.

2.3 Slice Thickness Effects on Defect Sensitivity

The thickness of the CT slice will also affect the detectability of small voids. The slice thickness will affect the SNR of Equation 2-1 by changing the intensity of the photons available at the detector. The modulation of a void, however, will change in relation to how it is partial volumed by the slice thickness. The modulation/noise (M/N) for a void can be estimated in a modification of Equation 2-1 such that:

$$M/N \propto \begin{cases} \mu[n_o w d t e^{-2\mu R}]^{1/2} & w < h \\ \mu(h/w)[n_o w d t e^{-2\mu R}]^{1/2} & w > h \end{cases} \qquad 2\text{-}2$$

where h is the height of the void in the object, w is the slice thickness, n_o is the photon intensity at the detector, and d is the detector width. As the slice thickness (w) increases, the photon intensity at the detectors increases so that the noise (N) will decrease. At small w, less than the height (h) of the void, the modulation (M) will not be affected by changing w. But, when w becomes larger than h, M will decrease by partial voluming. The effect of these offsetting mechanism is shown in Figure 2.3-1 for a theoretical model of a CT system.

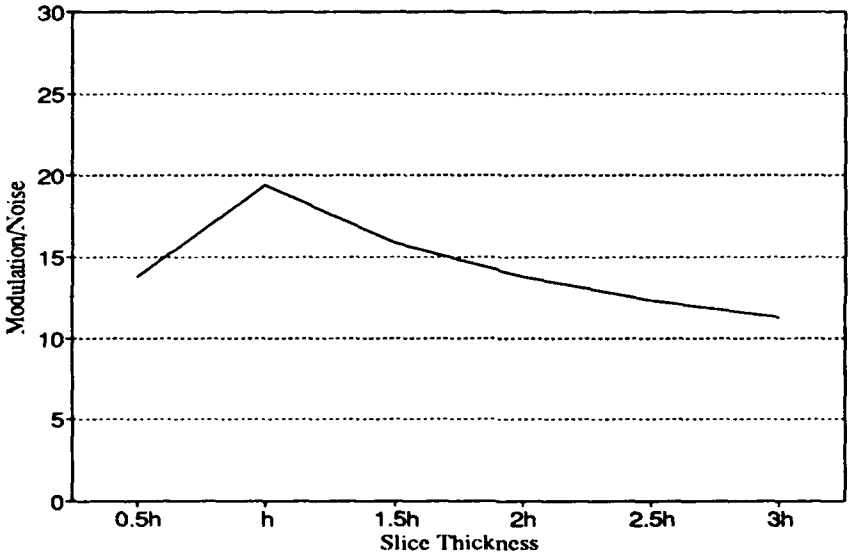

Figure 2.3-1 Theoretical model of modulation/noise versus slice thickness.

The effect of slice thickness can be measured empirically for a CT system using the IQI. Figure 2.3-2 shows the measurement of modulation of the CT value in the voids 0.012, 0.05, and 0.2 mm^3 divided by the noise, as a function of the slice thickness. The general shapes of the curves agree with theory for detectability as a function of slice thickness. However, the peak response is not at h, but at a slice thickness greater than h. Experiments on two different CT systems indicate this effect of peaking of the response at thickness settings larger than h. This appears to be due to an effective slice thickness at the object that is thinner than the CT system settings, limitations in the mechanical accuracy below 1 mm for large systems and perhaps other unaccounted effects. The experimental data provides an important means for optimizing defect sensitivity for a particular CT system.

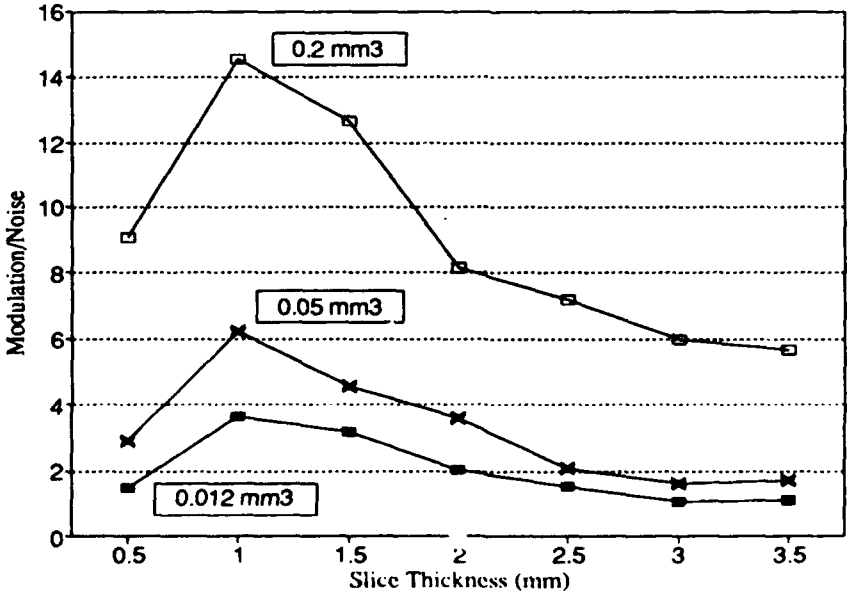

Figure 2.3-2 Modulation/noise versus slice thickness.

A thin slice thickness can provide excellent sensitivity to defects, but the thinner the slice, the more slices are required to cover the entire part. While CT can be used very effectively for high sensitivity in critical region inspection, this same sensitivity may be prohibitively time consuming to apply on 100 percent of the part, and so a less sensitive approach may be used in noncritical areas. Understanding the correlation between noise, part size, partial voluming and defect sensitivity can allow the prediction of CT system requirements to meet casting inspection needs.

2.4 IQI in a Complex Casting

The CT IQI fabricated for the casting analysis has been applied very effectively in the evaluation of a complex casting, by placing it in an internal cavity. Figure 2.4-1 is a photograph of a manifold casting. Although 100 percent radiographic inspection is required for this part, the actual inspection is 100 percent only in the sense that the entire part is covered by the exposure; all positions in the part cannot be practically monitored to the desired 2-2T penetrameter sensitivity.

Figure 2.4-2 shows a CT slice taken on the manifold. In the central cavity are two IQI's, one with a 0.25 mm (0.010 inch) disk thickness and one with a 0.125 mm (0.005 inch) disk thickness. Each disk contains holes of 1 mm (0.040 inch) and 0.5 mm (0.020 inch) diameter. The smallest disk thickness and hole diameter represents the minimum 2-2T requirement according to MIL-STD-453, (Inspection, Radiographic). This is the minimum detectable feature required for any thickness of material when using a radiographic inspection. In the CT case, this minimum sensitivity is valid for all regions in the CT slice, whether the material is thin or thick.

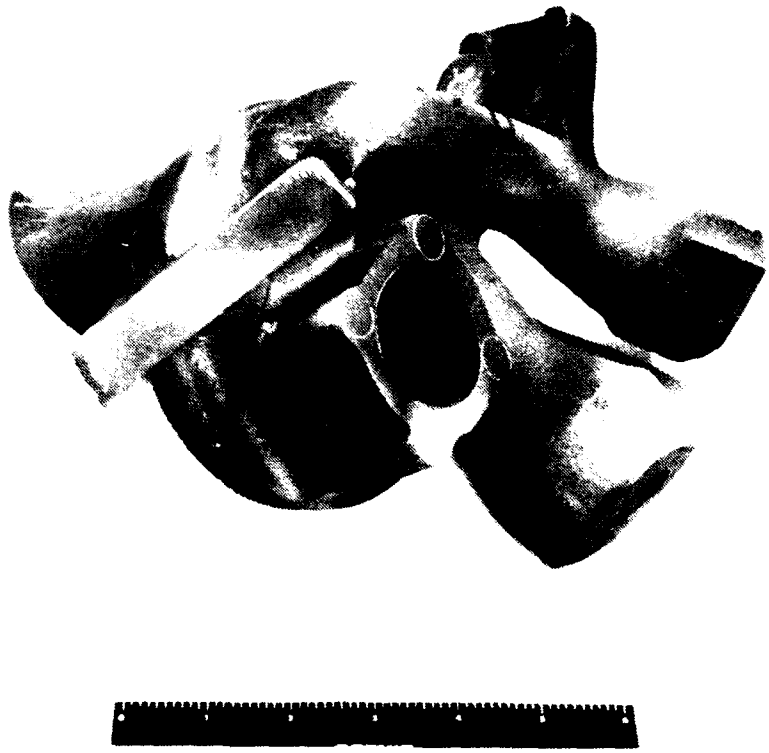

Figure 2.4-1 Photograph of a manifold casting (PID #030106).

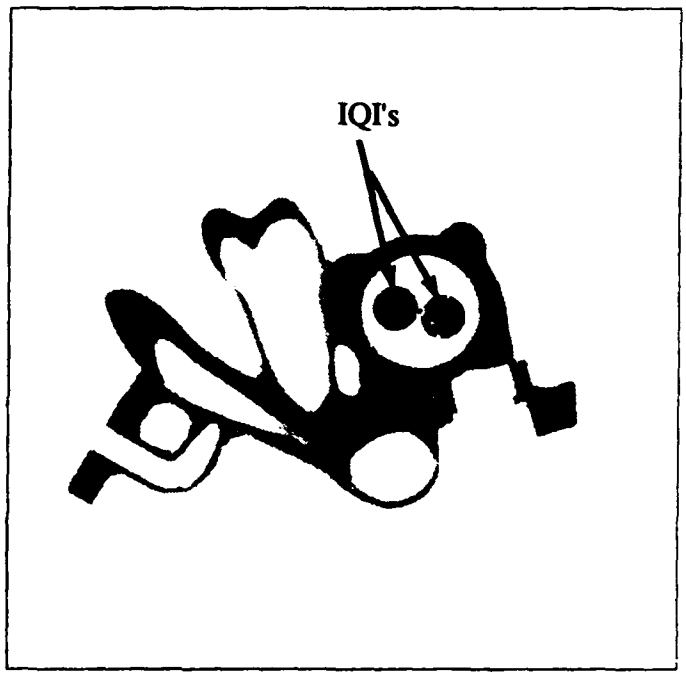

Figure 2.4-2 CT slice of the manifold casting with IQI's.

3.0 ENGINEERING ANALYSIS

3.1 Approach

Modern engineering has increasingly utilized the computer to create more complicated and sophisticated calculational models of the performance of structures under service conditions. The component model divides the structure in small elements (finite elements) in order to analyze the stress and strain that occur throughout the structure due to the load conditions. This finite element analysis (FEA) has become a routine tool for the structural engineer. The modeling is data intensive, therefore, the engineer will often utilize conservative strategies to create a model of the component that can be represented in the computer with as simplistic, yet realistic, a geometric approximation as possible.

An approach for analyzing a cast component using FEA and CT is shown in Figure 3.1-1. The process begins with the design of the component and the development of a finite element model of the component's application. The designer will run load tests of stress and strain of the component design using the computer model. When the component has been fabricated, it can be inspected by CT. The CT data can be converted to Initial Graphics Exchange Specification (IGES) file format. This allows the CT measurement of internal features to be input to the designer's finite element code. The designer will recalculate the stress and strain in the part under the load condition with the defect in place. This allows the engineer to establish whether or not a casting may be used in spite of any defects that may exist.

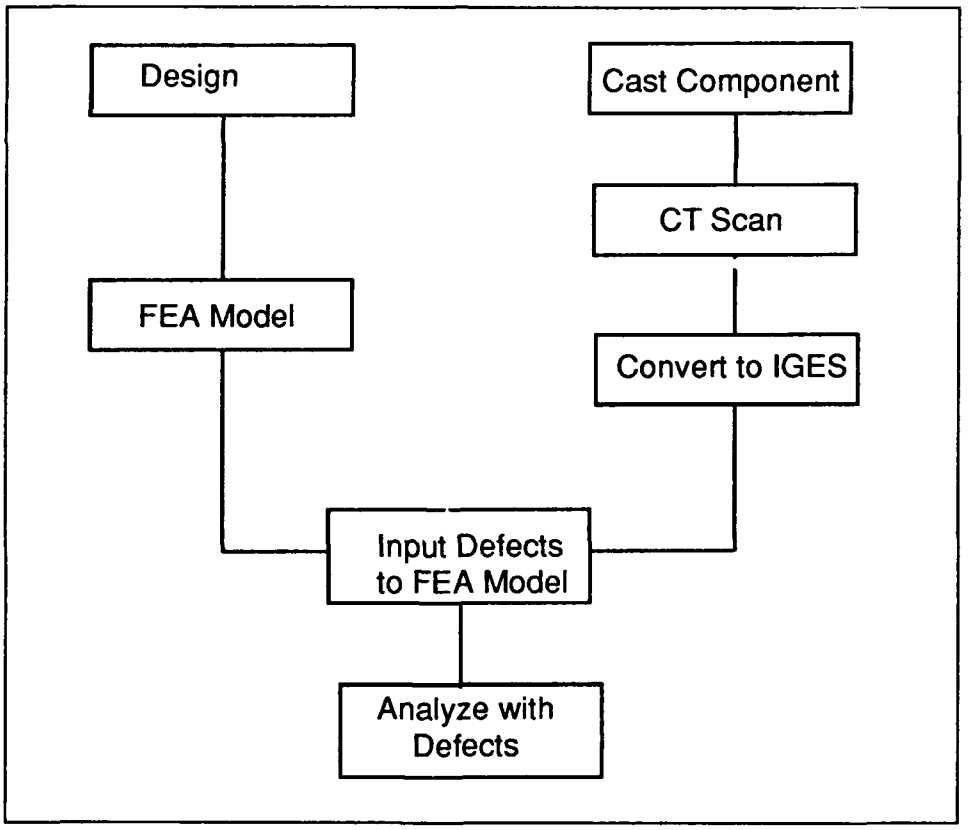

Figure 3.1-1 Approach for analyzing a cast component using FEA and CT.

3.2 Cast Component Example

In order to examine the possibility of using CT data in the engineering analysis of a component, an example of an aluminum cable drum casting has been selected. A photograph of the casting is shown in Figure 3.2-1. The casting is part of the cable linkage system in the trim mechanism for the control surface of an aircraft. The analysis is intended to be a generic representation of what could be done on any representative component and is not a specific detailed analysis of the operation of this cable drum casting design.

The drum castings have experienced very high rejection rates from penetrant and radiographic examination. However, over 2000 such units have been installed, many having service lives of more than 20 years, and none has ever failed in service. Such experience is not unknown for aircraft castings because they are conservatively designed and then inspected to quality standards that go beyond the requirement for their design application. Although this very high quality level requirement is admirable, the fact is, it has created excessive waste.

3.3 Computed Tomography

The casting shown in Figure 3.2-1 was rejected for radiographic indications which exceeded the acceptance criteria specified for the component. The component was designed Class 1, level B for inspection purposes, which is a relatively severe criteria [14]. The radiographs are compared to reference images for the decision on acceptability. The reference radiograph set demonstrates defects which vary in size, but there is no consideration of the depth of the defect and its impact on casting performance. A CT slice of the casting will, however, show the size of the defect in its true dimensions relative to the component material thickness, as shown in Figure 3.3-1. The CT image is a map of the defect in the plane of the component where the CT slice is taken. An enlargement of the defect area is shown in Figure 3.3-2.

The CT image can be converted to an IGES CAD/CAM file. In this process, the CT map of attenuation coefficients is converted to a line drawing of features of the component. Figure 3.3-3 is the IGES file drawing of the drum casting. The defect is shown with its size and location in the component defined.

Because the CT image is composed of points and intensities, the IGES file can be generated by connecting the points whose intensities represent the edges of the component features. However, the resulting IGES file will become very large relative to a CAD/CAM drawing file for the equivalent part. This file can be forty times larger than the CAD/CAM drawing file, depending the part shape and how simple a model is used. Compression routines can be utilized to reduce the IGES data. This is typically useful for reductions by factors of five to ten.

The IGES file, created from the CT data, can be utilized directly in a finite element analysis (FEA) code to perform the same analysis that might have been done on the original plan of the part. However, as noted earlier, because of the large size of the IGES file this may not be the most practical approach. Software programs can be written to interpolate and/or analyze the IGES file data to be equivalent to the conventional CAD/CAM finite element model descriptions, but such software is not currently available. If an existing model is available, the engineer can select from the IGES file data the particular region that is essential for evaluating performance. In the example of the drum casting, the flaw location and size are important. Figure 3.3-4 is an enlargement of the defect region. This information can be added to the FEA model that may have been created for the originally designed part and the calculations rerun. When it is appropriate, the engineer may enhance the size of the defect to provide a conservative estimate of the effect of the defect.

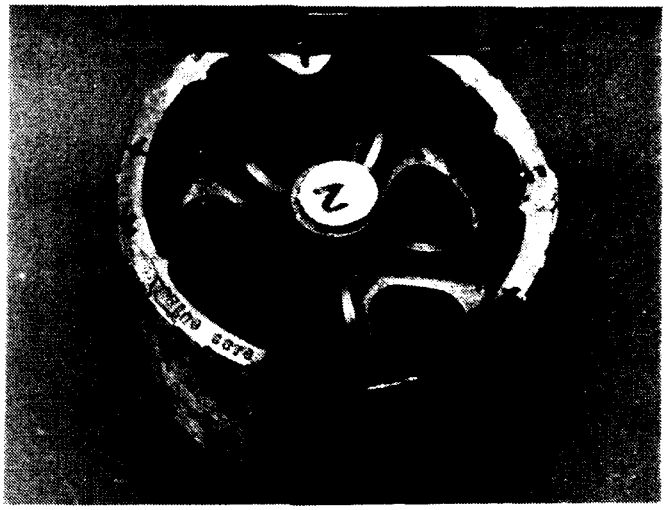

Figure 3.2-1 Photograph of an aluminum drum casting (PID #030176).

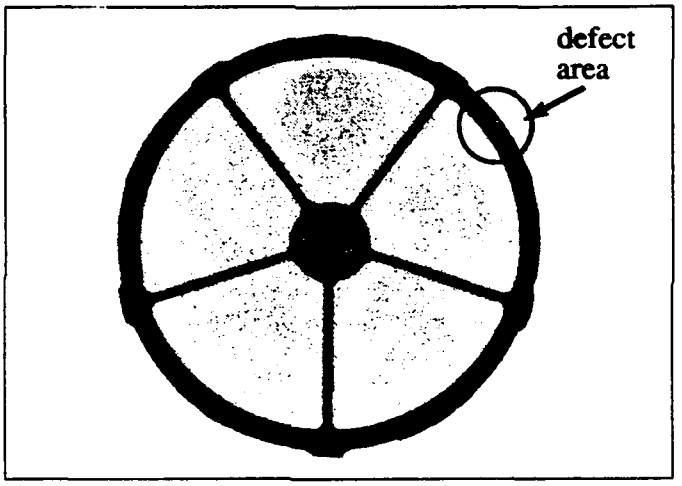

Figure 3.3-1 CT slice of a drum casting.

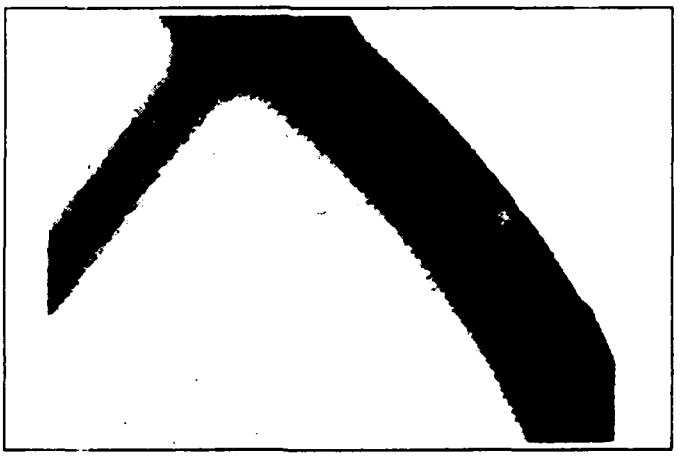

Figure 3.3-2 Enlargement of the defect area in the drum casting.

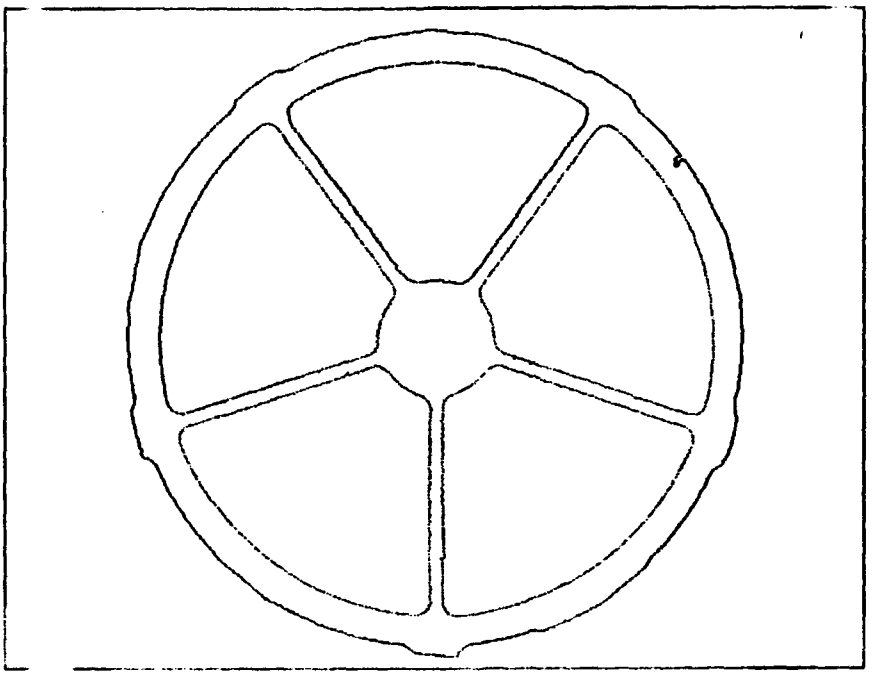

Figure 3.3-3 IGES file representation obtained from the CT image.

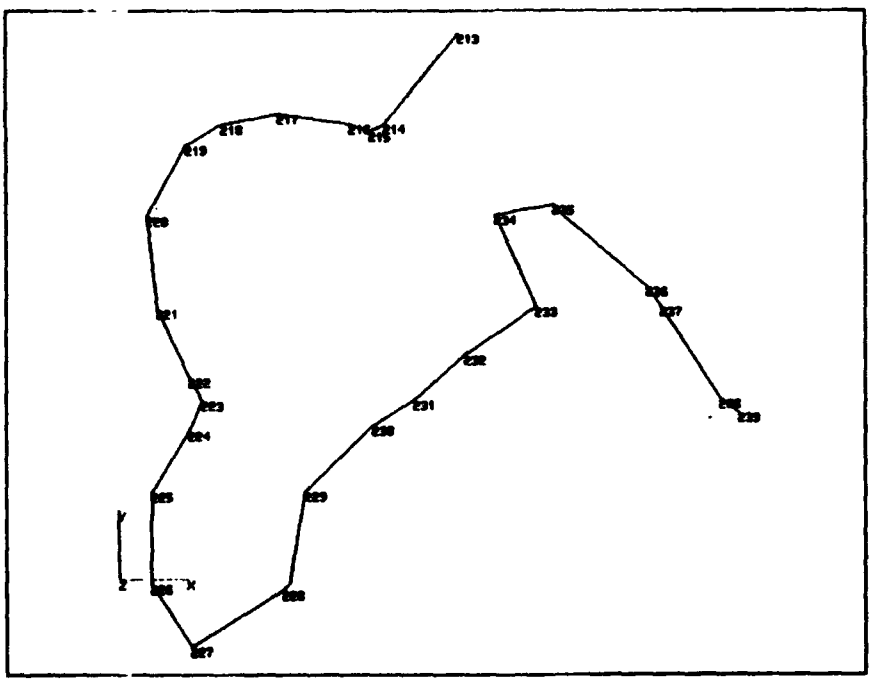

Figure 3.3-4 Defect representation for FEA model from IGES data.

3.4 Finite Element Model

The drum casting shown in Figure 3.2-1 can be modeled for engineering analysis as shown in Figure 3.4-1. The model considers the drum a symmetric part and uses a conservative approach by making the wall of the web and outside ring a uniform cross section corresponding to the thinnest portion in the casting. The actual casting will possess additional reinforcing. A load is applied to a quadrant of the drum simulating how the component may be loaded in service.

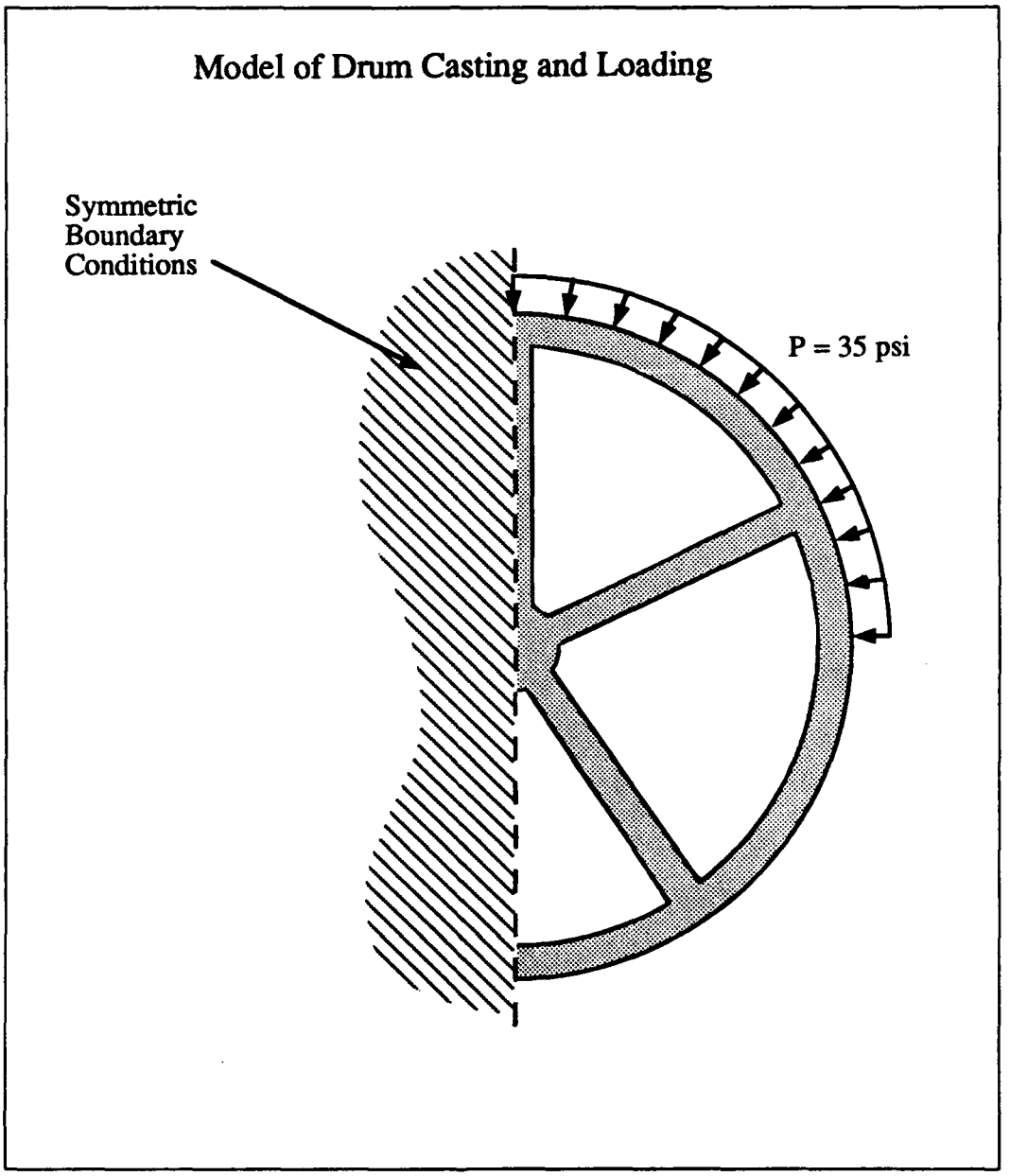

Figure 3.4-1 Diagram showing how an engineering analysis of a component would be made.

The geometry model of Figure 3.4-1 is input into a finite element code, which divides the interior of the part into small cells and calculates the internal stress and strain on the component

due to an external loading. Figure 3.4-2 shows the relative stress intensity distribution by contour lines in the region at the very top of the component. Figure 3.4-3 shows strain of the component due to the loading. The strain values have been amplified for the display. The displacement is only on the order of a few thousandths of an inch.

By using the information on the defect size and location from Figure 3.3-3 the engineer may insert the defect into the FEA model and rerun the calculations of stress and strain. Figure 3.4-4 shows the stress distribution in the component with the defect. The defect has been incorporated into the original "good" part file from the CT created IGES file and then has been intentionally enlarged to add conservatism to the engineering calculation. The FEA model with the defect uses a finer grid spacing for the calculations in the region near the defect. The local stresses are only 3 percent higher when the defect is present. Figure 3.4-5 shows the strain for the component model with the defect. With the defect present, the new strain calculation is only 2 percent higher. For this particular component design and loading example, the stress and strain on this component are not significantly altered by the presence of the defect, even though the defect is nearly half way through the wall. The implication from this analysis is that this casting example has a very conservative design.

Although the calculations have been performed on a computer, it is possible to also perform similar analysis by hand. When the geometry is relatively simple, this is the more economical approach. The size of the defect is measured from the CT data and the engineer calculates, by hand, a conservative estimate of the effect on the stress and strain in the component. Whether or not FEA is used depends then on the criticality of the component, the complexity of the design and the availability of the computational tools. A cost trade-off assessment will need to be made on which approach is best for any particular part.

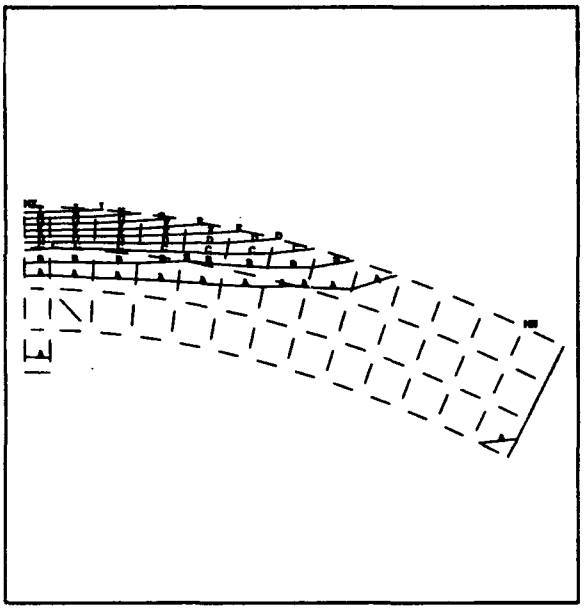

Figure 3.4-2 Stress analysis of a good casting.

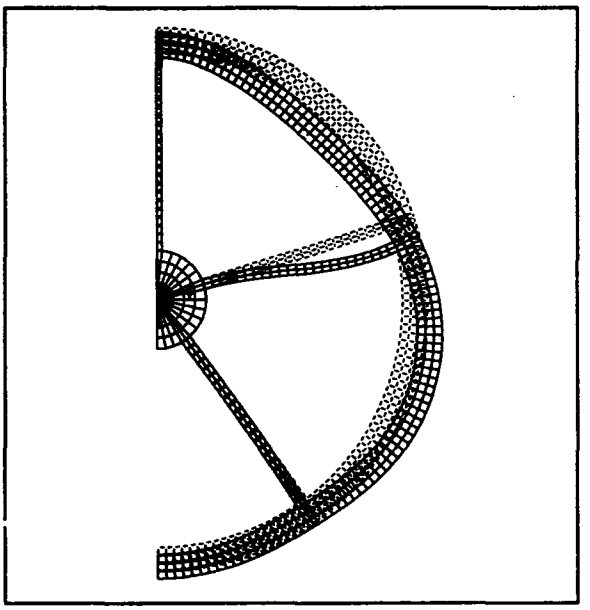

Figure 3.4-3 Strain analysis of a good casting.

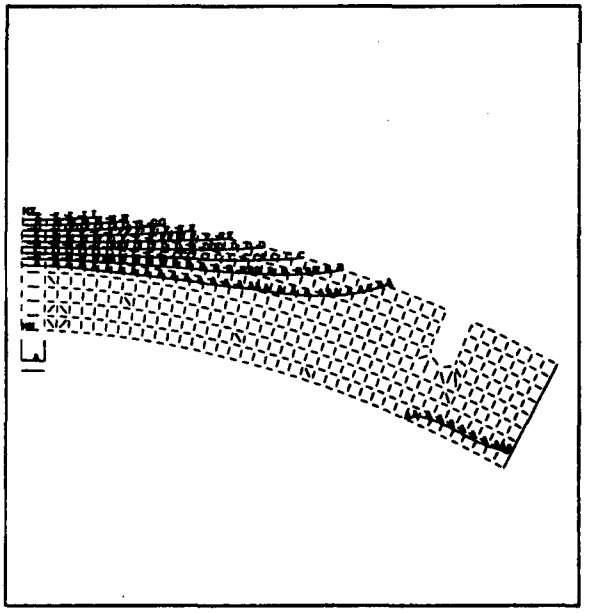

Figure 3.4-4 Stress analysis of a casting with a defect.

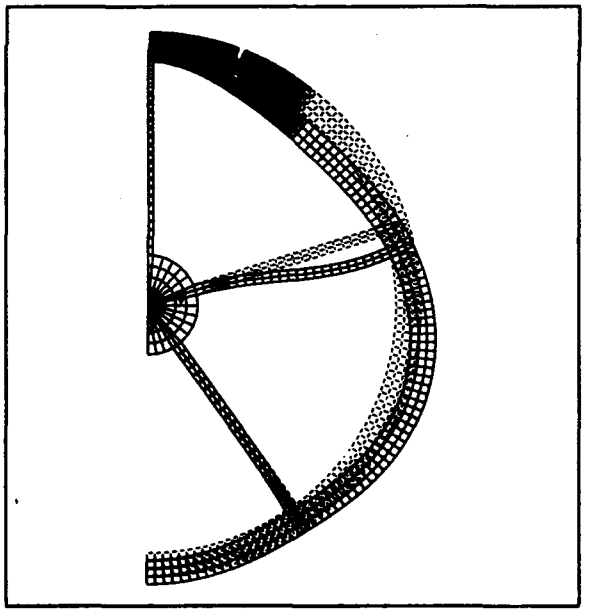

Figure 3.4-5 Strain analysis of a casting with a defect.

3.5 Summary of Engineering Analysis Study

The engineering analysis example shows that CT provides the link from inspection methodologies to engineering evaluation that can allow the engineer to design and utilize castings with greater confidence. The significant conclusions of this study which have broad implications for the use of castings are listed in Figure 3.5-1.

First, castings should be accepted or rejected on the basis of their material and structural properties being adequate for the job. Castings are generally overdesigned for strength. In many applications, stiffness rather than strength may be the critical design parameter. In the example, the rejection of the casting because of the indication of the flaw should not be for strength reasons; the casting will have adequate strength and stiffness despite large flaws. Second, the penetrant and radiographic standards most commonly applied unfortunately result in very high rejection rates for noncritical flaws. The strict inspection criteria may result in a cosmetically pleasing casting, but this comes at a considerable expense. A criteria often cited is to avoid porosity being brought to the surface in subsequent machining operations. But since strength is probably not the driving issue in the design, such porosity could be weld repaired, or with CT inspection, may be selectively avoided by knowledge of its specific location. Third, significant cost savings could result from a more enlightened approach to selecting the inspection criteria for castings. Typical scrap rates in the casting industry run 10 percent of the production, but have been known to climb to nearly 100 percent in aerospace castings such as the drum casting, for defects much less significant than that found in the example presented here. Also, aerospace castings are often passed at the foundry and rejected later during subsequent processes. These rejections often result in costs that exceed the cost of the component. Finally, CT provides the link in the inspection methodologies to engineering evaluation that can allow the engineer to design and utilize castings with greater confidence. Defects can be assessed for the critical location rather than full coverage with strict criteria. No castings are perfect. The defect sizes and their positions are the critical parameters. By combining engineering modeling with CT imaging the engineer can create a more cost effective product.

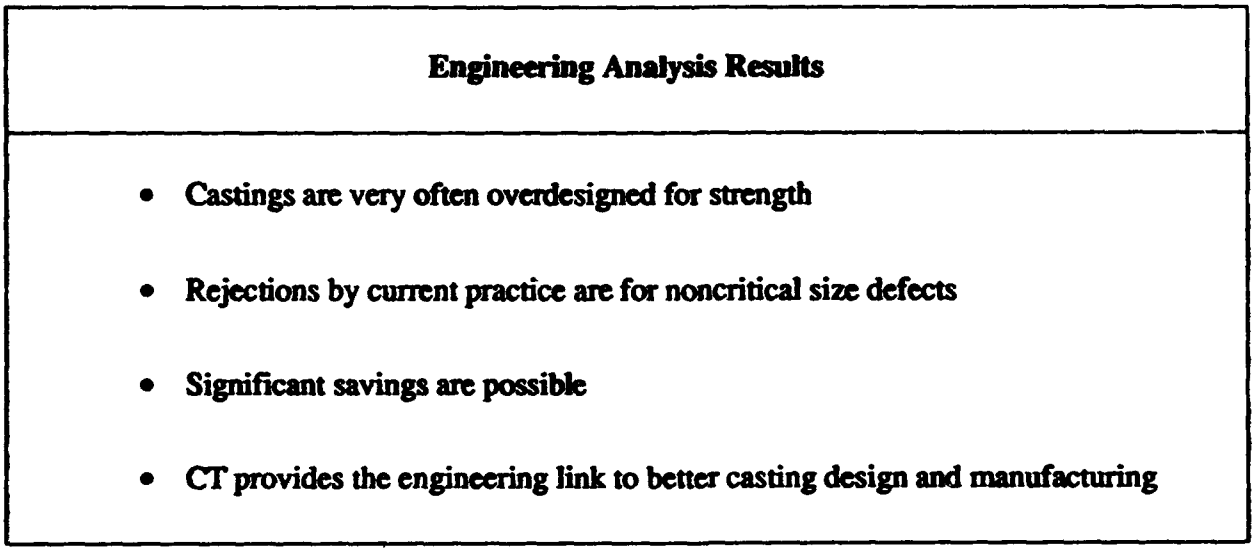

Figure 3.5-1 Issues identified in the engineering analysis of castings.

4.0 DIMENSIONAL MEASUREMENTS

Dimensional measurements of finished parts are very important in casting manufacture. Internal measurements of shapes and sizes of features, and clearances are particularly difficult to acquire in a complex casting. CT provides a nondestructive method to measure internal dimensions with considerable accuracy. A test phantom for determining the dimensional measurement precision of CT has been tested using two approaches for measurement of clearance dimensions from CT images: 1) fifty percent threshold and 2) gap shape. The simplest approach works very well for large dimensional measures and a more complex approach yields good results when small gaps must be measured. CT image data can be processed to solve for the position of edges very accurately because of the large set of views that are used to compose the pixel intensity, creating very accurate intermediate measurement values at edges.

4.1 Test Phantom, PID #000801

Figure 4.1-1 is a drawing of a small (40 mm (1.6 inch) diameter x 25 mm (1 inch) thick) aluminum dimension phantom developed in an earlier CTAD task assignment [4]. The phantom contains machined surfaces, bolted together to form designed gaps of 3.0, 1.0, 0.5, 0.25 and 0.12 mm (0.12, 0.04, 0.02, 0.01 and 0.005 inch). Using an optical method, the gap width measurements were 3.01, 1.02, 0.50, 0.23, and 0.09 mm (0.118, 0.04, 0.02, 0.009 and 0.004 inch). The phantom also contains both axial and side drilled holes of 3, 1 and 0.5 mm (0.12, 0.04, 0.02 inch) diameter. Figure 4.1-2 is a photograph of the phantom (CTAD part identification number 000801). A CT slice through this phantom can be analyzed to determine small gap measurement accuracy and precision from CT system configurations.

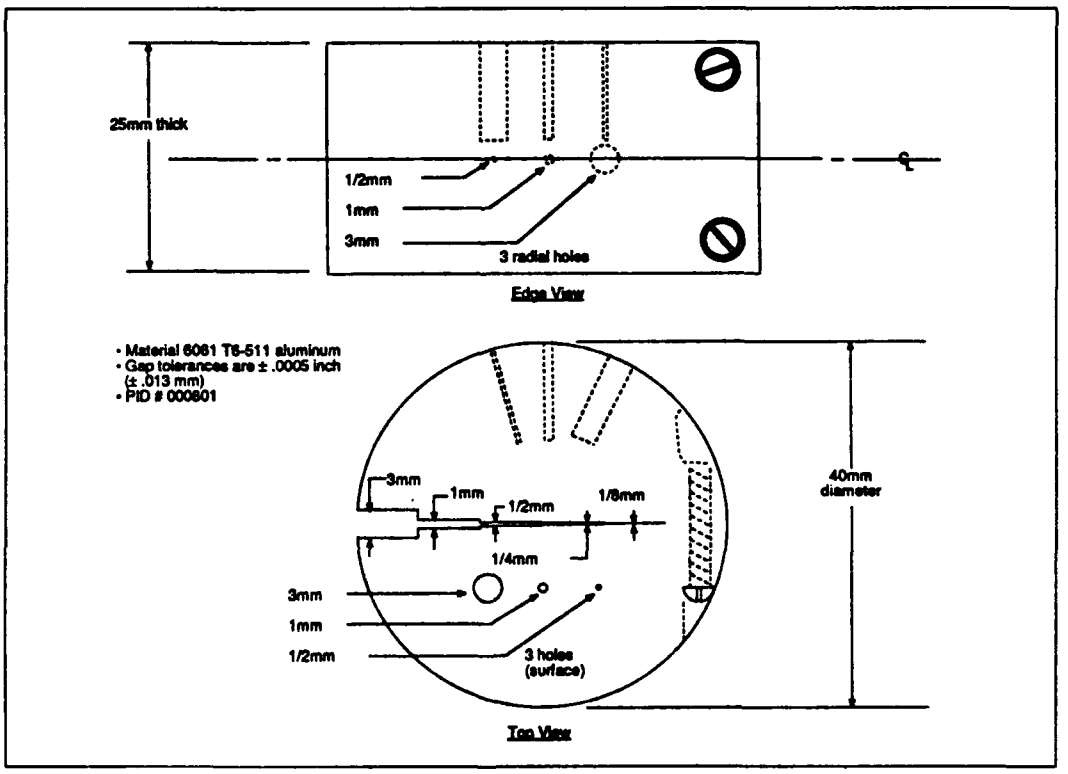

Figure 4.1-1 Drawing of aluminum dimensional phantom.

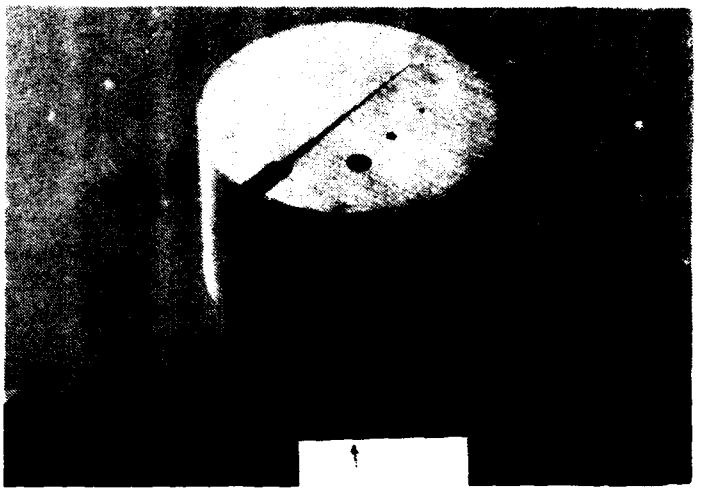

Figure 4.1-2 Photograph of the aluminum dimensional phantom (PID #000801).

4.2 Measurement Techniques

Dimensional measurement accuracy and precision of a CT system operational configuration will be a function of the resolution, contrast and noise in the reconstructed image. A CT slice of the test phantom that cuts across the gaps provides an image that can be analyzed for dimensional accuracy. Line traces taken across gaps from the CT image of the test phantom are shown in Figure 4.2-1.

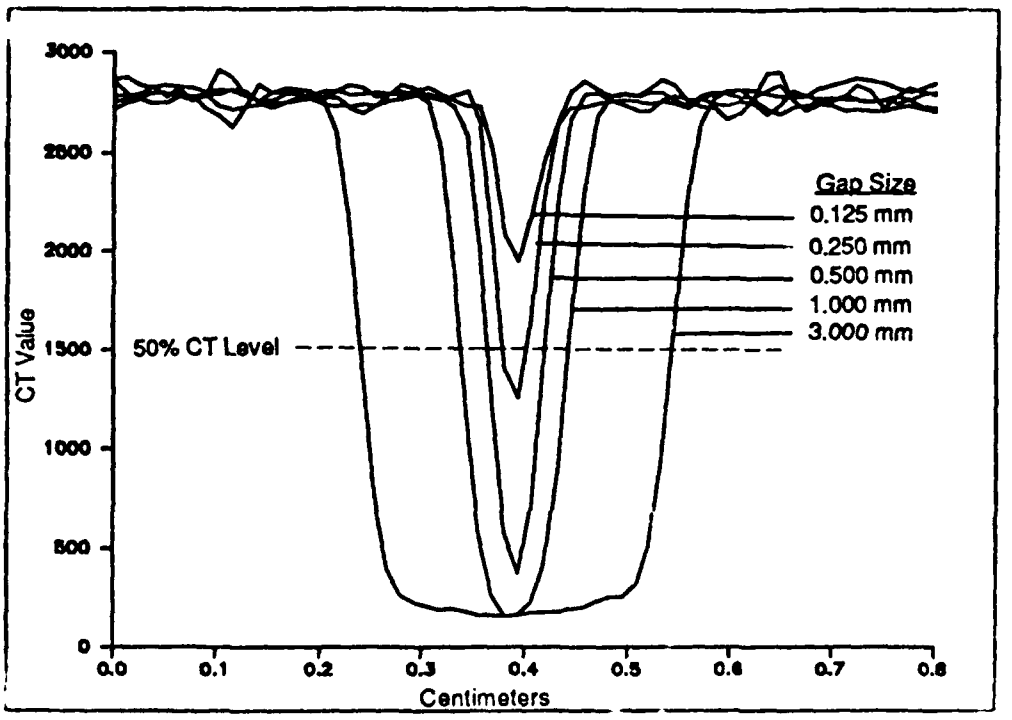

Figure 4.2-1 Line traces across the dimensional phantom gaps showing the decrease in modulation with decreasing gap width from CT system #3.

As the gaps decrease in size, the modulation of the gap becomes smaller. This effect can be mathematically described as the convolution of the point spread function of the CT image with the gap size. A system configuration with inherently greater resolution than another will show a higher modulation of the gap. In general, the pixel size used in the CT image should at least correspond to the inherent resolution of the CT system, and preferably it should be somewhat finer. If the pixel size is larger than the inherent resolution capability then the contrast across the gap will be reduced due to smoothing. However, depending on the data analysis approach, the gap measurement accuracy may not necessarily be lost.

In the simplest application of the test phantom the CT slice is taken perpendicular to the faces of the gap. Under this condition the CT slice thickness will not affect the edge shape. However, if in practice the CT slice is angled, for any reason, with respect to gap faces, then the slice thickness will cause a blurring of the line traces due to the partial voluming of the edge of the gap in the CT imaging volume element or voxel. As the CT slice becomes thicker, this partially voluming effect becomes more significant. On an angled gap, a thin CT slice might be preferred. Depending on the information available on the gap orientation and CT slice width, corrections may be made to regain accuracy in the dimensional measurement.

4.2.1 Fifty Percent Threshold

A simple approach to dimensional measurements between edges is to define a threshold CT number to be the edge. Then image pixel coordinate measurements are made between thresholded edges and converted to dimensional measurements. Table 4.2-1 is a table of dimensional measurements on the test phantom using four different CT systems and the 50 percent threshold level. The four CT systems have a range of inherent resolution roughly covering <0.25 to 0.5 mm. The CT slices have been taken perpendicular to the gap faces for these measurements. The 50 percent threshold level approach, of course, cannot allow for calculation of the dimension when the gap modulation decreased below the 50 percent level. This will occur approximately when the inherent resolution of the CT system is on the order of the gap size.

Table 4.2-1 Gap width measurement by the 50 percent threshold technique.

Optically Measured Gap Width	CT System 1		CT System #2		CT System #3	CT System #4
(mm)	Alone	Inserted	Alone	Inserted	Alone	Alone
3.01	2.99	3.08	2.95	2.98	3.00	3.01
1.02	1.10	1.16	0.99	0.96	1.02	0.97
0.50	0.62	0.65	0.22	0.04	0.51	-
0.23	0.31	0.16	-	-	0.15	-
0.09	-	-	-	-	-	-

In two cases shown in the table of data, the phantom was inserted into a larger part as discussed in an earlier task assignment report [4]. Under this condition, the noise in the CT image is increased resulting in a loss of accuracy and precision.

The results of Table 4.2-1 are obtained by averaging the gap dimension obtained from a number of line traces (20 to 120 depending on the CT system) across the gap. Table 4.2-2 show the standard deviation of the line trace measurements. The results indicate that accurate and precise measurements, better than 0.050 mm (0.002 inch), are possible in the high contrast large gap regions. This measurement capability is equally applicable to measurements across large regions of the component. When the gap begins to approximate the resolution of the CT system however, this 50 percent threshold approach shows highly inaccurate measurements or no measurement value. None of the CT system configurations could use this technique for the 0.12 mm gap.

Table 4.2-2 Standard deviation of line trace gap width measurement using the 50 percent threshold technique.

Optically Measured Gap Width	CT System #1		CT System #2		CT System #3	CT System #4
(mm)	Alone	Inserted	Alone	Inserted	Alone	Alone
3.01	0.02	0.05	0.02	0.02	0.01	0.05
1.02	0.02	0.10	0.004	0.04	0.01	0.06
0.50	0.02	0.16	0.02	0.04	0.01	-
0.23	0.02	0.11	-	-	0.03	-
0.09	-	-	-	-	-	-

The individual line trace approach across the gaps, as applied here, is useful to indicate the variation found in CT system configurations of varying inherent resolution. In practice it is important to remember that a gap implies that there is length to the feature. Measurements of the gap width should therefore not be obtained from single line traces but rather by averaging line traces along the gap length in order to obtain the most accurate measurement.

Preliminary experiments have also been run with the gap angled at 30 degrees to the CT slice. Under these conditions the gap width measured by the 50 percent threshold technique increased by 1/cos(30) as should be expected. As the CT slice thickness increased however, the modulation in the gap decreased because of partial voluming in the CT voxel. This places a limitation on the minimum size of the angled gap that can be measured with a thick CT slice using the 50 percent threshold. The accuracy of measurements on large gaps, with small, known anglulation to the CT slice should be very good. As the gap becomes narrower, the measurement will depend upon the understanding of the gap orientation, the gap size relative to the inherent resolution of the CT system and the slice thickness.

4.2.2 Gap Shape

As noted earlier, the decrease in modulation across a gap can be represented by the convolution of the point spread function of the CT imaging system with the feature to be measured, in this case, a gap. By knowing the point spread function it is possible to deconvolve its effects in order to improve the accuracy of a gap measurement. The value of actual density (ρ_a) across the gap at position δ whose origin is the center of the gap will be given by:

$$\rho_a(\delta) = \begin{cases} \rho_m & \text{for } \delta < -G/2 \\ \rho_g & \text{for } -G/2 \le \delta \le G/2 \\ \rho_m & \text{for } \delta > G/2 \end{cases} \qquad 4\text{-}1$$

where ρ_m is the density of the base material, ρ_g is the density of the gap material and G is the gap width. The general solution for the observed density (ρ_o) at position Δ in the image space will be:

$$\rho_o(\Delta) = \frac{\int_{-H/2}^{H/2} S(\delta-\Delta)\rho_a(\delta)d\delta}{\int_{-H/2}^{H/2} S(\delta-\Delta)d\delta} \qquad 4\text{-}2$$

where H is a distance larger than G and S is the point spread function of the CT imaging system. Combining equations 4-1 and 4-2 yields:

$$\rho_o(\Delta) = \frac{\rho_m\int_{-H/2}^{-G/2} S(\delta-\Delta)d\delta + \rho_g\int_{-G/2}^{G/2} S(\delta-\Delta)d\delta + \rho_m\int_{G/2}^{H/2} S(\delta-\Delta)d\delta}{\int_{-H/2}^{H/2} S(\delta-\Delta)d\delta} \qquad 4\text{-}3$$

Equation 4-3 contains all known information, except for the gap width (G). By choosing G such that the value of the expression:

$$\int_{-H/2}^{H/2} \left[\rho_o(\Delta) - A(\Delta)\right]^2 d\Delta \qquad 4\text{-}4$$

is a minimum, where $A(\Delta)$ is the right hand side of equation 4-3, then the best estimate of the gap will be achieved. The value $\rho_o(\Delta)$ should be obtained by averaging line traces along the gap (tangent to the gap edges).

The expression 4-4 is theoretically valid for large gaps where the value of the CT density in the gap reaches the minimum value. However, in practice many CT systems have beam hardening or other image density variations which, over a very large gap, may introduce errors. Provided the line spread function is symmetric the value of the expression 4-4 will be a minimum when G is the distance between the 50 percent threshold levels on the edges of the gap. Thus, the general solution for gap measurements based on shape predicts that the 50 percent threshold should be correct for large distance measurements.

A special case of Equation 4-3 can be applied to the gap measurement of small gaps in the aluminum phantom where the gap does not have full modulation. For this special case, the ρ_o at the center of the gap (H = 0) is calculated for a number of values of G. The resulting table of ρ_o values as a function of G values is then used as a lookup table. For this procedure to be successful, a point spread function for each CT system must be available. It can be obtained by

differentiating an edge spread function, which is available in the CT image of the phantom. The measured CT density value in the image is compared to the calculations in the table and the estimated gap size is given. This analytical approach allows gap measurements to be made that are below the inherent resolution of the CT system configuration.

Table 4.2-3 shows the measurement results of this gap shape analysis for the test phantom 0.5, 0.25 and 0.12 mm wide gaps, which do not have full modulation in the line traces from the CT images. Excellent accuracy is obtained with any of the system configurations for the cases tested.

Table 4.2-3 Gap width measurement by the gap shape technique.

Optically Measured Gap Width	CT System #1	CT System #2		CT System #3
(mm)	Alone	Alone	Inserted	Alone
0.50	0.55	0.52	0.66	0.54
0.23	0.30	0.26	0.25	0.27
0.09	0.12	0.12	0.06	0.12

Equation 4-1 through 4-3 should be applicable to gaps that are angled with respect to the CT slice. The partial voluming of the CT slice voxel on the gap wall can be accounted for in the S term of the equations. These equations can also be generalized even further for interfaced between dissimilar materials as well such that:

$$\rho_a(\delta) = \begin{cases} \rho_{m1} & \text{for } \delta < -G/2 \\ \rho_{m2} & \text{for } -G/2 \le \delta \le G/2 \\ \rho_{m3} & \text{for } \delta > G/2 \end{cases} \qquad 4\text{-}5$$

where ρ_{m1} is material 1, ρ_{m2} is the interface material (air for a gap) and ρ_{m3} is a third material. This approach can therefore be used on a variety of multiple material interfaces where fine gaps need to be evaluated.

5.0 STEREOLITHOGRAPHY

5.1 Stereolithography

Stereolithography is a process for creating three-dimensional plastic parts from CAD/CAM data. This particular manufacturing process, developed by 3D SYSTEMS, Inc. [15], uses an ultraviolet laser beam and a photosensitive polymer bath. The laser beam is made to follow a path which describes a single plane from the solid model of component in a CAD system. The beam polymerizes the resin in a bath. The now partially cured layer is lowered on a table so that fresh liquid material flows over the top to form a new layer above. Now this new layer can be polymerized by the laser beam in the form of the next higher plane in the solid model. As successive layers are added, a 3D part is fabricated out of plastic.

The major application of Stereolithography is in rapid prototyping of test articles from CAD/CAM drawings for engineering evaluation of form and fit. Stereolithography is not the only method being developed for rapid prototyping [16], however, it is the leading free-form manufacturing technology at this time [17].

5.2 Casting Example

The nature of Stereolithography makes it a natural partner for CT data. Both technologies deal with slice information of a three-dimensional body. Stereolithography offers the opportunity to build models of components from CT data. The Stereolithography model can be made to the scale of the test article, or reduced or enlarged for the desired display of information. For the analysis of castings, Stereolithography can provide models of internal cavities, configurations, and defects that are detected by CT scanning.

A demonstration of this capability has been performed using a casting sample with an internal shrinkage cavity. Figure 5.2-1 is a photograph of the test coupon containing a shrinkage cavity. The coupon (PID #030119) is approximately 30 mm x 25 mm x 15 mm (1.2 inch x 1 inch x 0.6 inch) that has been removed from a larger aluminum casting. A series of 200 CT slices were taken over the part and a 3D computer model of the part was made from the data [4]. Figure 5.2-2 shows the 3D presentation of the coupon with the shrinkage cavity acquired from CT data.

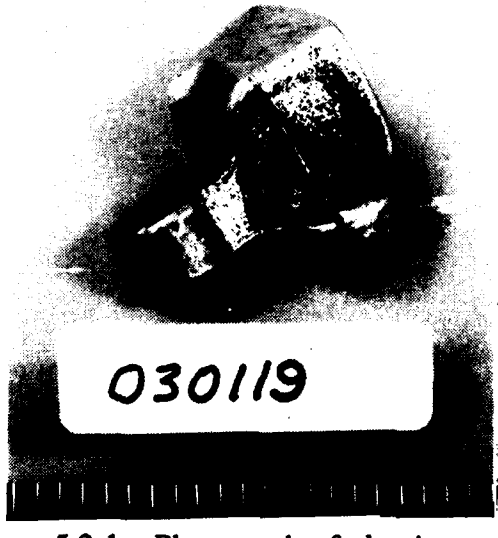

Figure 5.2-1 Photograph of aluminum test coupon containing shrinkage cavity (PID #030119).

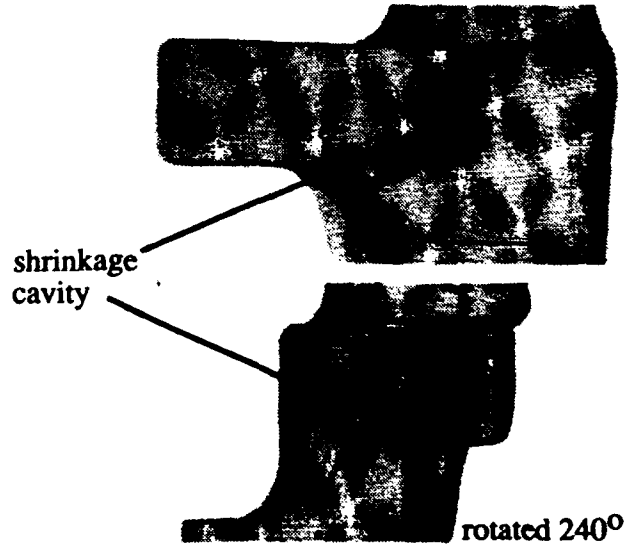

Figure 5.2-2 3D image rendering of the test coupon from CT images.

5.3 Results

Figure 5.3-1 shows two flow diagrams for conversion of the CT data to create a Stereolithography model. In the first case the CT data is thresholded and contours are created at the threshold level selected. The contours are reviewed by an individual and modified if necessary. The contours are then converted to an IGES file input for transfer to a CAD system. Figure 5.3-2 shows the IGES model of the part from a CAD system. In the second version of the flow diagram the CT data is directly converted to a ".sli" file format that the stereolithography system can use to create each plane, or equivalent slice, in the plastic model. This process has been developed at the University of Kentucky for medical CT data sets and can be applied to industrial parts [18].

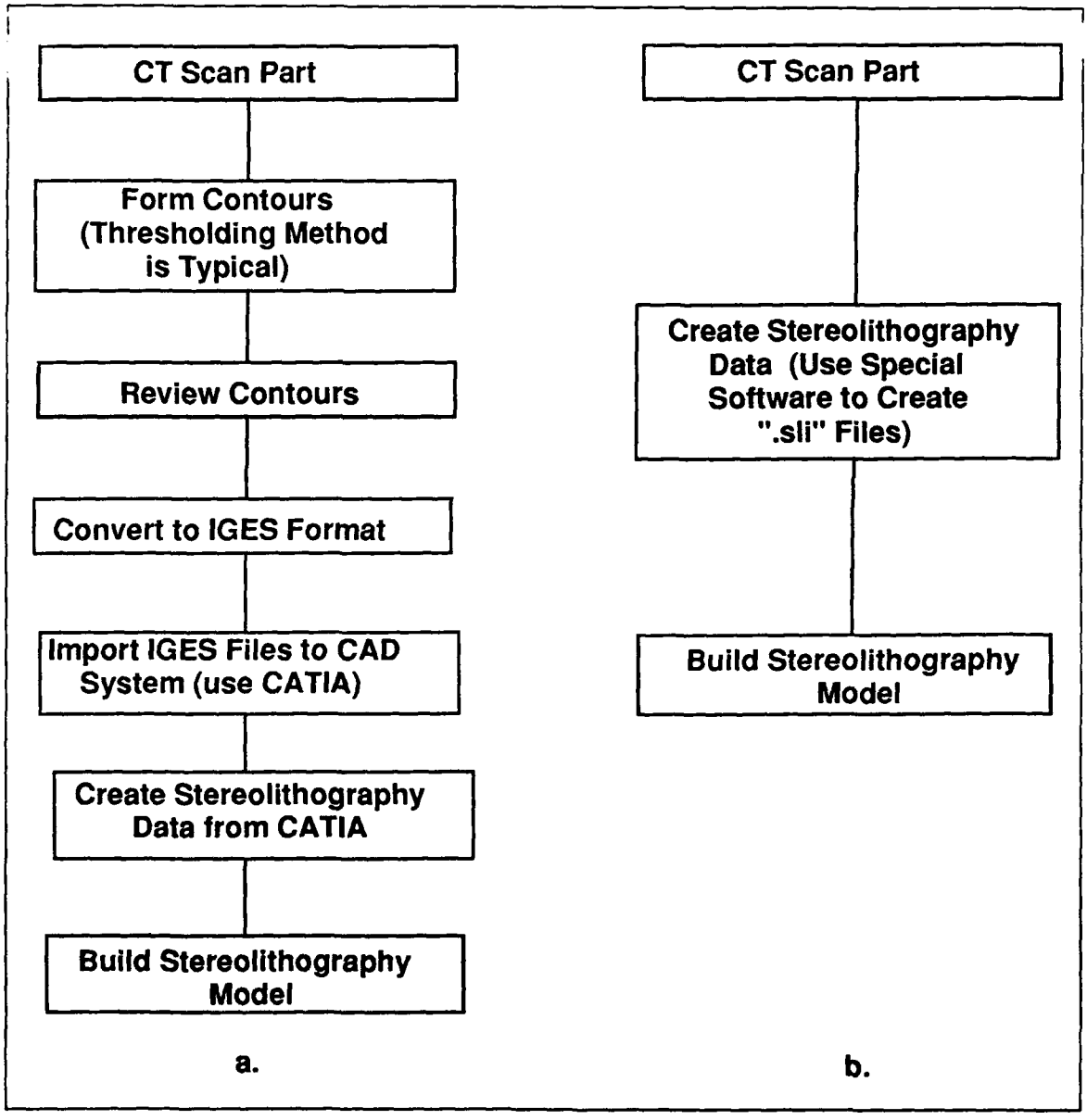

Figure 5.3-1 Flow diagram of data transfer from CT to Stereolithography by two approaches, a) conversion to CAD system and then to Stereolithography, and b) direct conversion to Stereolithography.

When access to the direct conversion of CT data to ".sli" files is available, this is the most direct and cost effective approach. Thus, the original CT data which was used to create the Figure 5.3-1 image was sent to the University of Kentucky. The data was converted to ".sli" format and a model constructed. Because the area of interest was an internal cavity, the 3D data set was divided along a path that separated the part at the internal cavity so that two matching pieces could be created which would have a portion of the cavity in each half. The process of actually constructing the model involves a significant level of expertise in understanding the part to be built and the parameters of the Stereolithography system. For example, if the part to be constructed has an overhang, then support structure must be added to the ".sli" files so that the overhang will be formed properly and not collapse in the liquid bath. The resin material will also influence the selection of the laser scanning data spacing, scanning speed and cure. The set of ".sli" files created by the University of Kentucky was transmitted to Boeing where additional models were constructed. Some modification of the ".sli" files and system parameters was necessary in order for the models to be constructed on a different stereolithography system with a different resin bath.

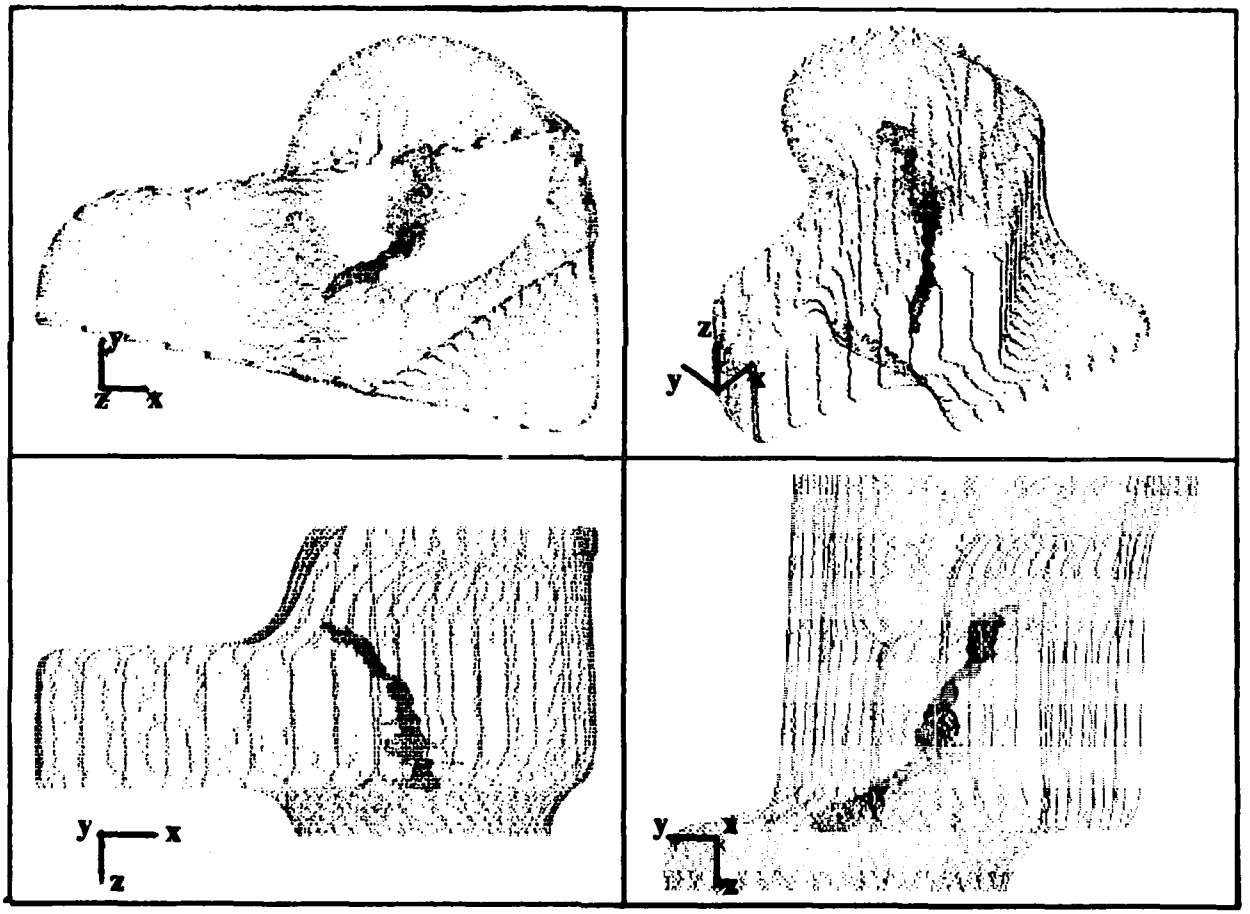

Figure 5.3-2 Computer graphics 3D renderings of the casting after IGES transfer into a computer design system.

Figure 5.3-3 is a photograph of the plastic model created by Stereolithography and the original component. The model is nominally a 2X version of the original sample constructed as a mirror of the original part. The Stereolithography model was created in two parts that fit together to represent the orignal component. Figure 5.3-4 shows the Stereolithography model opened to reveal the internal defect cavity. The model provides a useful tool for demonstration of internal physical effects in components. Multiple samples can be readily made in the resin bath at once. The Stereolithography production labor time for this example was approximately 12 hours to create 4 complete models.

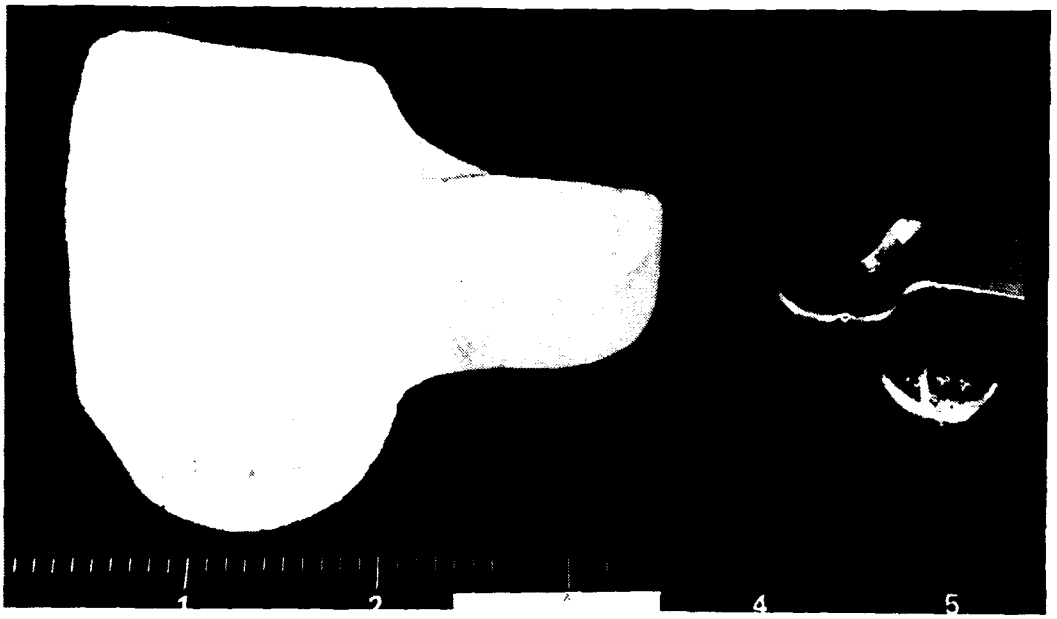

Figure 5.3-3 Photograph of the Stereolithography model and the PID #030119 part.

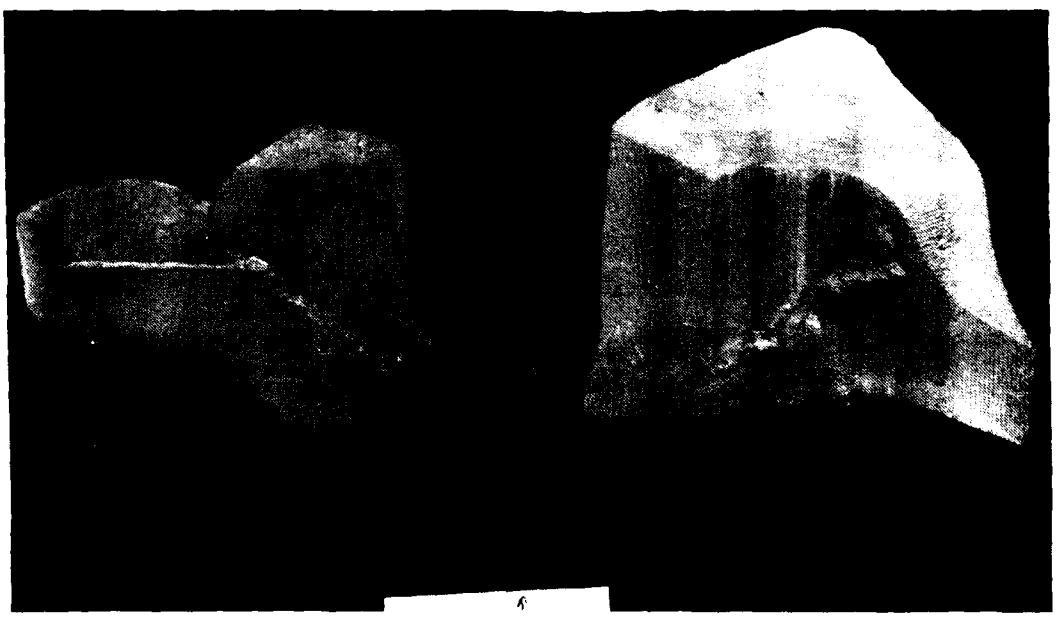

Figure 5.3-4 Photograph of the Stereolithography model opened to display the internal defect cavity.

6.0 CONCLUSIONS AND RECOMMENDATIONS

6.1 Conclusions

The quantitative measurement capability of CT has been shown to be effective for the engineering analysis of castings. CT provides the link in the inspection methodologies to engineering evaluation that can allow the engineer to design and utilize castings with greater confidence. CT sensitivity to anomaly sizes has been measured by the use of image quality indicators. CT imaging may be as sensitive to volumetric defects as radiographic inspection, with respect to MIL-STD-453 requirements. The sensitivity of a CT system, as a function of object size and system operating parameters, can be established and monitored.

The accuracy and precision of dimensional measurements for features in castings can be excellent. Dimensional measurements to better than 0.050 mm (0.002 inch) are fairly easy to achieve with the CT system configurations tested. Using appropriate techniques, measurements that have previously been considered to be beyond the inherent resolution of the CT system can be made, as demonstrated for small gaps of 0.5 to 0.12 mm (0.020 to 0.005 inch). This measurement capability has been obtained on a small (40 mm (1.6 inch) diameter) test sample, but the methodology of dimensional measurements should provide accuracies on much larger parts as well that are in the range of 1 part in 10,000.

The three-dimensional location and definition of flaws, obtained from CT evaluation of castings, have been input into finite element engineering models to analyze the performance as a function of the casting condition. In the case of one particular object type, a cable drum casting, the results indicate that castings are very conservatively designed for strength. This was confirmed experimentally as well on a rejected cable drum casting tested to over 3 times operational load without failure. Thus, rejections associated with this casting have been for noncritical flaw sizes. This story is common for castings in the aerospace industry. A significant cost savings in the manufacture of castings and their increased aerospace application are possible when quantitative evaluation, such as CT, and fitness-for-service criteria are used.

The data sets from CT scanning have been converted to CAD/CAM files and input to Stereolithography system to build a 3D plastic model of a part. CT can be effectively used to reverse engineer and reconstruct components for visualization as part of the engineering analysis. This reverse engineering capability can also allow drawings to be made of components in their as-built condition or for which drawings do not exist.

6.2 Recommendations

The CTAD effort recommends that casting designers utilize CT in the development and analysis of castings. By using CT imaging and critical flaw size criteria developed from engineering models, it is possible to evaluate castings more appropriately and effectively than is presently practiced. It is recommended as well that future work look into the potential of CT measurements to correlate with performance measurements on castings.

The potential economic return in using CT for reverse engineering should be explored by the Air Force for logistical support of the existing fleet. Reverse engineering offers cost savings in maintaining systems for which replacement costs could be high. By generating drawings and models, the risk involved in remanufacture is reduced with a subsequent overall reduction in bid cost. The economics of using CT for both internal and external dimensional measurements and generation of the component drawings appears to be of considerable value. This needs to be quantified under future task assignments and compared to obtaining the information by conventional means.

7.0 REFERENCES

1. R. H. Bossi and G. E. Georgeson, "X-ray Computed Tomography of Full Scale Castings," WL-TR-91-4049

2. R. H. Bossi, R. J. Kruse and B. W. Knutson, "Computed Tomography of Electronics," WRDC-TR-89-4112, December 1989.

3. R. H. Bossi, J. L. Cline and B. W. Knutson, "Computed Tomography of Thermal Batteries and Other Closed Systems," WRDC-TR-89-4113, December 1989.

4. R. H. Bossi, J. L. Cline, E. G. Costello and B. W. Knutson, "X-Ray Computed Tomography of Castings," WRDC-TR-89-4138, March 1990.

5. R. H. Bossi, K. K. Cooprider, and G. E. Georgeson, X-Ray Computed Tomography of Composites," WRDC-TR-90-4014, July 1990.

6. P. Burstein and R. H. Bossi, "A Guide to Computed Tomography System Specifications," WRDC-TR-90-4026, August 1990.

7. R. H. Bossi and R. J. Kruse, "X-ray Tomographic Inspection of Printed Wiring Assemblies and Electrical Components," WRDC-TR-90-4091, October 1990.

8. ASTM E 1025-84 - "Standard Practice for Hole-Type Image Quality Indicators Used for Radiography."

9. S. Hughes, "Nonuniformity of Spatial Resolution in Computed Tomography Scanners," *Materials Evaluation*, 48, May 1990, pp. 562-565.

10. ASTM "Standard Guide for Computed Tomography (CT) Imaging," to be released.

11. M. J. Dennis, "Industrial Computed Tomography," Metals Handbook Ninth Edition, Volume 17 Nondestructive Evaluation and Quality Control. ASM, Metals Park, OH (1989).

12. H. H. Barrett and W. Swindell, *Radiological Imaging, The Theory of Image Formation, Detection, and Processing*, Volume 2, Academic Press, NY, (1981).

13. E. McCullough, J. Payne, H. Baker, R. Hattery, P. Sheedy, D. Stephens and E. Gedgaudus, "Performance Evaluation and Quality Assurance of Computed Tomography Scanners, with Illustrations from EMI, ACTA and Delta Scanners," *Radiology*, Vol 120, July 1976, pp. 173-178.

14. MIL-STD-2175, "Castings, Classification and Inspection of."

15. C. Hull, "Stereolithography in the 1990's," 3D System, Inc., Valencia, CA.

16. S. Ashley, "Rapid Prototyping Systems," *Mechanical Engineering*, April 1991, pp. 34-43

17. "Computers in Engineering," Supplement to *Aerospace Engineering*, Vol. 11, No. 7, July, 1991, p. 10.

18. Charles Fisher, Wenner-Gren Laboratory, University of Kentucky, Rose St., Lexington, KY 40506, (606)-257-3040.

APPENDIX - CT Image Quality Indicator

Image quality indicators (IQI's) provide a means of quantitatively assessing the performance of imaging systems. Figure A-1 is a schematic drawing of the IQI developed for this casting study. The CT IQI is composed a 19 mm (0.75 inch) diameter disk of selectable thickness, containing 2 or 3 holes, with cylindrical shims of the same material on both sides of the thin disk. The IQI thus contains cylindrical voids of a height equivalent to the disk thickness and diameters of the holes. The diameters chosen are the same as the smallest diameters required by MIL-STD-453C "Military Standard for Inspection, Radiographic" for the 1T, 2T and 4T holes used in radiographic penetrameters, i.e., 1.0 mm (0.040 inch), 0.50 mm (0.020 inch) and 0.25 mm (0.010 inch). For the case of a 0.25 mm (0.010 inch) thick disk these equate to volumetric void sizes of 0.2, 0.05, and 0.012 mm^3 respectively.

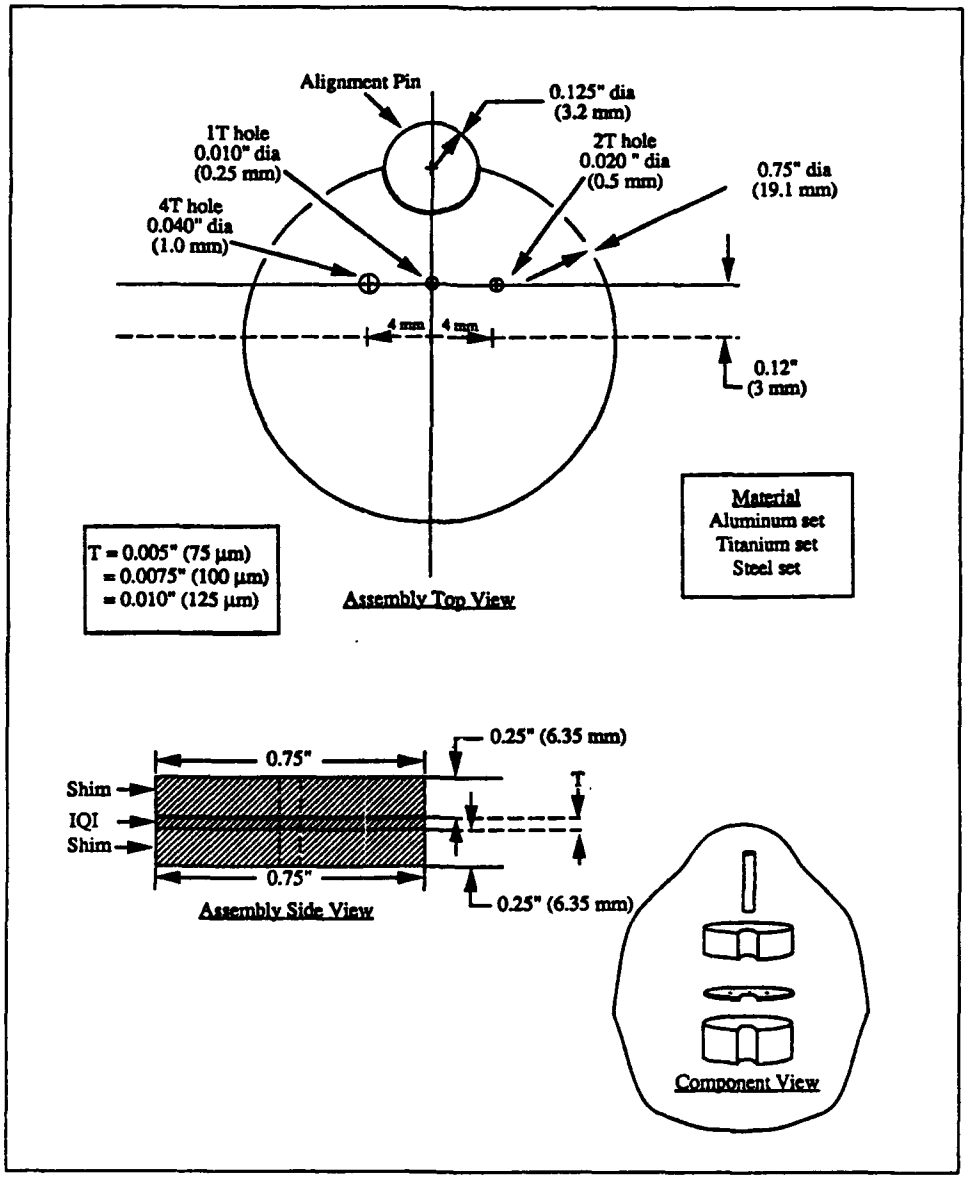

Figure A-1 Schematic drawing of the CT IQI developed for the casting study.

In order for the IQI to be useful, the CT slice must be taken such that it covers the plane of the disk. The CT slice may be thicker than the disk and still be sensitive to the voids. Each cylinder has an angled slot cut into it to assist in centering the X-ray slice on the IQI. The partial volume effect of the slots allow one to calculate the actual X-ray beam slice width and location. Figure A-2 illustrates how this takes place. Figure A-3a shows a 0.25 mm (0.01 inch) thick CT slice located 1 mm (0.04 inch) high (above the disk) demonstrating a CT slice that is off-center. Figure A-3b shows a slice that is centered on the IQI.

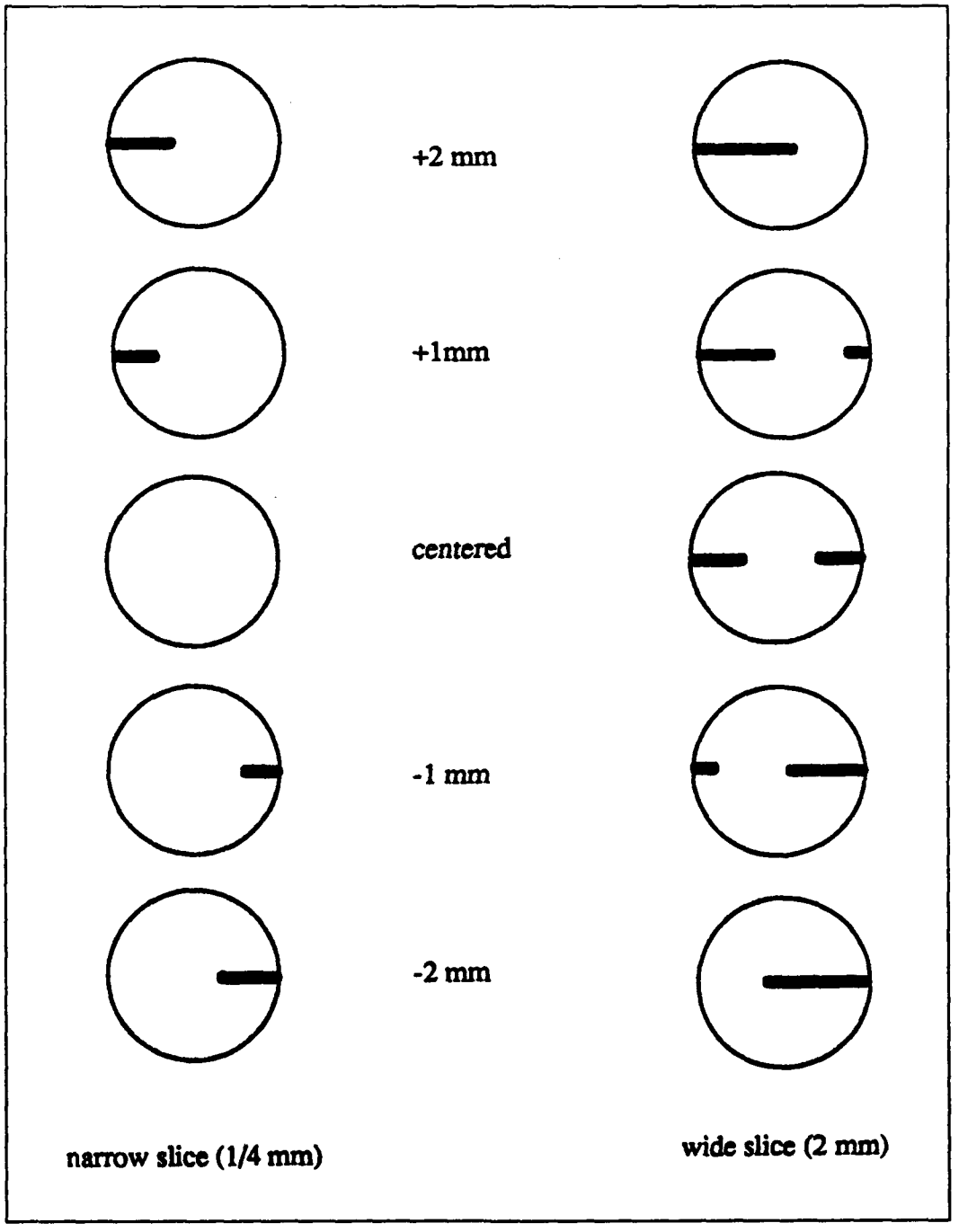

Figure A-2 Illustration of centering the CT slice using the slots in the IQI.

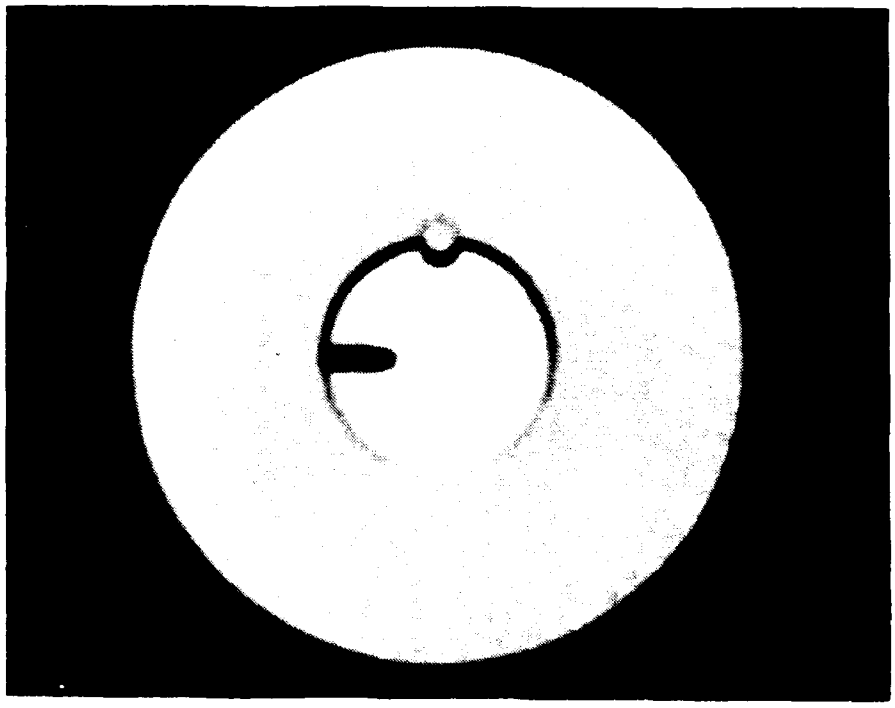

a)

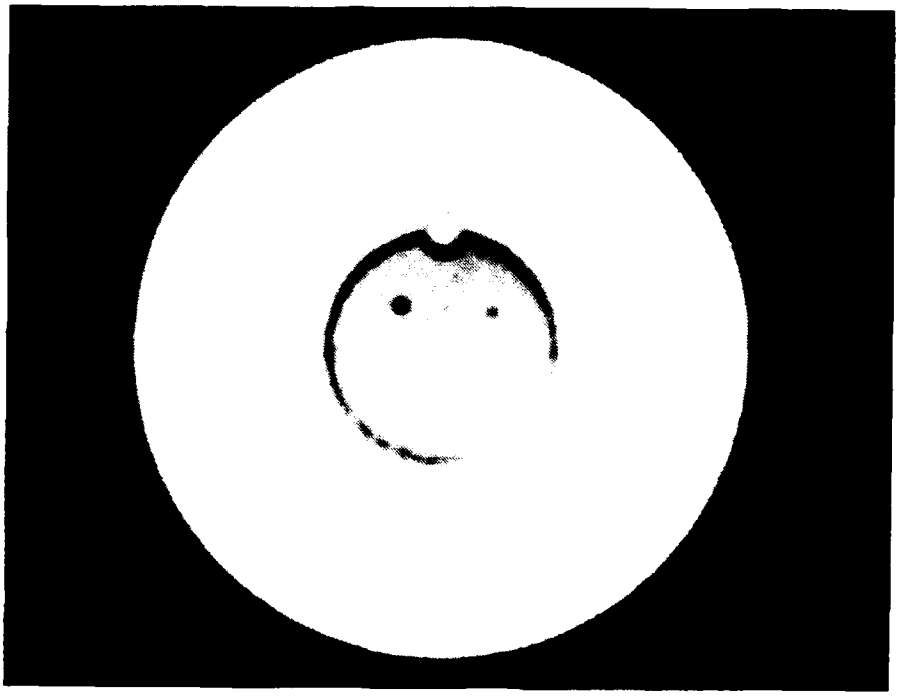

b)

Figure A-3 CT images of the IQI a) a 0.25 mm thick CT slice located 1 mm high on the IQI, b) a slice that is centered on the IQI.

 ☆U.S. GOVERNMENT PRINTING OFFICE: 1992 - 648-127/62201